1582 Pre-Biopsy PSA and Highest Percentage of Cancer (hPCA) on Prostate Biopsy Can Adequately Predict Upgrading of Gleason Score (GS) on Subsequent Prostatectomy: A Single Institution Study in a Cohort of Patient with GS 6

G Venkataraman, K Rycyna, RC Flanigan, EM Wojcik. Loyola University Medical Center, Maywood, IL.

Background: Several studies have shown that Gleason Score (GS) is a strong predictor of adverse outcomes after prostatectomy for prostate cancer. Specifically, upgrading of tumors scored as GS=6 on initial biopsy, to a GS>6 on subsequent prostatectomy imposes a significant burden, given the aggressive behavior of cancers with GS>6. The current study was performed to identify demographic and biopsy variables that might predict such upgrading to GS>6 in a cohort of patients with GS=6.

Design: A total of 647 prostate cancer patients diagnosed between 1999-2003 who had concurrent prostatectomy data and biopsy data available were identified in our database. From this, we selected a cohort of 184 patients with a biopsy GS=6. Clinical data including age, pre-biopsy PSA, and biopsy variables including percentage of positive biopsy sites (PPBS), highest percentage of cancer at any single site (hPCA), and presence of high-grade prostatic intra-epithelial neoplasia (HGPIN) or perineural invasion (PNI) were extracted. Multivariate logistic regression models (LRM) using a forward Wald method were constructed in SPSS 13 (Chicago, IL) to identify factors predictive of upgrading to GS>6.

Results: From a total of 184 patients with GS=6, ninety-two cases (92) were upgraded to GS>6. Among the upgraded cases, 90 (97.8%) had upgrading to GS 7, and 1 each (1.1%) had upgrading to GS 8 and GS 9. LRM identified a model with two variables that had a statistically significant ability to predict upgrading, including pre-biopsy PSA (Odds Ratio 8.66; 2.03-37.49, 95% CI) and hPCA (Odds Ratio 1.03, 1.01-1.05, 95% CI). This two-parameter model yielded a predictive accuracy of 62.2%. None of the other variables (age, PPBS, presence of HGPIN or PNI) were included in the final model.

Conclusions: The utilization of PSA and highest percentage of cancer at any single biopsy site will significantly help in decreasing the incidence of upgrading of GS on subsequent prostatectomy in a cohort of patient with GS=6 on the initial biopsy. This information may aid treating physicians in more precise risk stratification of patients with prostate cancer prior to therapeutic interventions.

1583 Quality Assurance in Anatomic Pathology: Correlation of Intraoperative Consultation with Final Diagnosis in 2812 Specimens

VA White, MJ Trotter. Vancouver Coastal Health Research Institute, University of British Columbia, Vancouver, BC, Canada; Calgary Laboratory Services, University of Calgary, Calgary, AB, Canada.

Background: The correlation of intraoperative consultation with the final diagnosis on permanent sections should form an integral part of quality assurance activities in the anatomic pathology lab. Despite this, publications on this topic are uncommon and there are no data from Canadian institutions. We aimed to completely review correlation of intraoperative consultation with final diagnoses over a 1-year period in a large general hospital setting in a major Canadian city.

Design: One pathologist reviewed all surgical pathology cases at Calgary Laboratory Services that had an intraoperative consultation from June 2004-May 2005 to determine the intraoperative diagnosis, final diagnosis, correlation between the two, site of request, pathological process, types of disagreement and reasons for disagreement. The agreement rates were calculated as percent agreement, sensitivity/specificity, positive and negative predictive values, likelihood ratios, Youden J and the kappa statistic with 95% confidence intervals.

Results: 2812 specimens had an intraoperative consultation, of which 109 were discordant and 122 were deferred to permanent sections. The percent agreement was 96.12% (95%CI 95.41, 96.84) with a kappa statistic of 0.92 (95%CI 0.90, 0.93). The other measures of agreement were similarly high. Lymph nodes for metastases (427), thyroid/parathyroid (401) and CNS/PNS (378) specimens were most frequently sent for intraoperative consultation and the latter two tissue types accounted for the greatest number of disagreements. The most common pathological processes encountered were presence/typing of a neoplasm (1093) and assessment of margins (698), both of which accounted for the largest number of disagreements. Disagreements were most frequently due to interpretive (64) and gross sampling errors (33); false negative disagreements were 3 times as common as false positives.

Conclusions: By all measures used, the intraoperative consultation was an excellent diagnostic test. Limited pathological processes encountered in specific groups of specimens produced most of the disagreements. Two categories of error were responsible for the majority of the disagreements, which were most commonly false negatives. These results suggest specific measures that can be taken to reduce the number of discrepancies.

1584 Frozen Sections on Basal Cell Carcinomas: Improving Accuracy of Margin Evaluation and Assessment of Clinical Impact

AL Wilson, E Kilner, EC Wang, WG Watkin. Evanston Northwestern Healthcare, Evanston, IL.

Background: Basal cell carcinoma (BCC) is the most common form of skin cancer. While metastatic spread and death from disease are rare, there is morbidity associated with these lesions in the form of local recurrence. Frozen section (FS) examination is often used to evaluate the margins of these tumors when arising in locations where skin-sparing is paramount. Unfortunately, the accuracy of FS is sub-optimal with false negative (FN) rates as high as 15% reported. We studied a cohort of specimens from patients with BCC who had FS examination for margin status, and determined which factors may have contributed to FN FS diagnosis. Additionally, we evaluated the subsequent actions of the surgeons in response to positive margins and recurrence rates.

Design: Between 1/2000 and 10/2000, 181 consective cases of BCC which had FS examination were reviewed. Factors which might impact FS accuracy were evaluated: specimen size, tumor site, pathological subtype, distance from margin, quality of FS slide, % of specimen frozen, and number of FS slides prepared per specimen. In cases with positive margins (either true positive or false negative FS), we documented whether the margin was re-excised . We also documented the presence of tumor recurrence.

Results: The FN rate was 13.3% (n=24). Good FS quality (all margins evaluable, p=0.04) and greater distance from surgical margin on FS (p=0.004) correlated with a lower FN rate. Fewer slides made during FS, smaller specimen size, and greater % of specimen frozen were also associated with lower FN rates, but these were not statistically significant. Patients with FN FS had a higher recurrence rate (RR) than those with accurate FS (29.2% vs 13%,p=0.04). Specimens with positive margins on either FS or permanent section only (FN) were reexcised 57.5% of the time. The RR of reexcised positive margins was not significantly different than those that were not reexcised.

Conclusions: Only close surgical margins and sub-optimal FS quality had a statistically significant relation to FN FS. Error rates in BCC frozen section might be reduced if close margins are considered positive and re-excised and FS quality is enhanced. However, the failure of surgeons to consistently act on positive margins and the inability of reexcision to impact significantly BCC recurrence calls into question the need for FS evaluation.

1585 Mis-Identification Defects in the Analytic Phase of Surgical Pathology Work Processes

RJ Zarbo, RC Varney, R D'Angelo, JM Tuthill. Henry Ford Health System, Detroit, MI.

Background: Accuracy of patient identification is a national patient safety goal for laboratories requiring evaluation and monitoring of processes involved in accuracy of patient and sample identification at specimen collection, analysis and resulting (CAP TLC.11100). In surgical pathology (SP), these activities encompass the total test process from pre-analytic (specimen collection, labeling, transport) through analytic (specimen accession, gross, histology, slide interpretation, report generation) to post-analytic (report transmittal, interpretation). The frequency of mis-identification within the SP domain (internal mis-ID defects) is unknown. We defined these defects within the analytic phase of testing , as a prelude to implementing barcode specified work processes in SP.

Design: Internal mis-ID defects were documented over 3 weeks in July 2006 by 59 personnel in the SP laboratory of Henry Ford Hospital. Defects were categorized by part (lab tag, specimen container, block, slide, report) and further by root cause (patient name, label, medical record number, accession, specimen part, slide level and recut numbers, tissue and diagnosis). Defect frequencies and sigma values were calculated for error opportunities (cases, specimen parts, blocks and slides).

Results: From 2694 cases, there were 4413 specimen parts, 8776 blocks and 14,270 slides. 45 (1.67%) cases had mis-ID defects with 10 defects in accessioning, 5 in blocks and 30 in slides. Defect rate per million opportunities was on average 4.4 sigma or 1856 per million. Accessioning defects were due to case number, medical record number, part type, laterality, tissue site and manual block generation. 3 block defects were from specimen grossing and 2 at the microtome. 26 of 30 slide mis-ID defects had incorrect labels and in 4 cases pathologists transposed slide numbers. Internal mis-ID defects resulted in 4 amended reports, 2 of which resulted in changed diagnoses. Defects required 159 hours of rework to correct, equal to an annualized manpower increment of 1.3 full time equivalent employees.

Conclusions: This is the first documentation of frequency and root causes of identification defects occurring within the work processes of SP. All mis-ID defects would have been potentially addressed by use of an integrated identification system of barcoded lab tags, blocks and slides. This defect frequency supports investment in technology to address these potentially critical errors, the cost of which may be offset by avoidance of labor required to correct defects.

Techniques

1586 Rapid Quantitative Measurment of Gene Expression in Formalin-Fixed Tissues and LCM Samples without RNA Purification Using the QuantiGene® Branched-Chain DNA Assay

A Allen, D McLerran, J Davies, B Vessella, G McMaster, A Kristal, BS Knudsen. Fred Hutchinson Cancer Center, Seattle, WA; U Washington, Seattle, WA; Panomics, Fremont, CA.

Background: The difficulty in measuring RNA concentrations in FFPE tissues arises from extensive fragmentation and crosslinking of RNA after formalin fixation. The QuantiGene® (QG) assay does not require RNA purification and relies on cooperative hybridization: its probe design and non-enzymatic RNA capture and detection overcome the adverse effects of formalin fixation. The QG technology uses an ELISA-type format and is ideally suited for simple, rapid and high-throughput sample preparation and measurement of gene expression panels in FFPE tissue homogenates.

Design: Duplicate samples from 10 different xenografts were snap frozen or fixed in formalin. RNA was measured either after isolation (pRNA) or after solubilization in a tissue homogenization buffer (thRNA). Probe sets for capture of formalin-fixed (FF) RNA were specifically designed for short RNA fragments. To validate the QG assay, we measured the expression of six genes in 20 samples in parallel by qPCR, Agilent 2100 bioanalyzer and QG assay and obtained correlation coefficients directly from the variance components model. To evaluate the reliability of the QG assay, we determined the intraclass correlation coefficient (ICC). Laser capture microdissection (LCM) was performed with the Veritas® instrument.

Results: Measurements using the QG assay for RNA preparations from FF tissues were highly reproducible, with ICCs of six genes ranging between 0.84 and 0.97. The correlation coefficients for measurements of gene expression by QG assay in FF and

frozen tissues compared to qPCR measurements of frozen tissues were between 0.53 and 0.93 and between 0.22 and 0.93, respectively. In contrast, the correlation coefficients of qPCR measurements ranged between -0.33 and 0.72. The sensitivity of the QG assay in FF tissues was comparable to qPCR for pRNA, however it was significantly increased for tissue homogenates. The QG assay accurately measures 28S and18S RNA and 18S DNA in fewer than 5000 cells. Measuring a gene expression profile in LCM tissues that distinguishes cancer from normal epithelium provided the expected increases of gene expression in laser captured prostate cancer glands.

Conclusions: The QuantiGene® assay permits measurements of RNA in tissue homogenates without RNA isolation and provides a rapid workflow and better reproducibility, accuracy and sensitivity than PCR-based methods.

1587 Evaluation of Phi29-Based Whole Genome Amplification for Microarray-Based Comparative Genomic Hybridisation

E Arriola, MBK Lambros, C Jones, T Dexter, A Mackay, DSP Tan, N Tamber, K Fenwick, A Ashworth, M Dowsett, JS Reis Filho. Institute of Cancer Research, London, United Kingdom; Institute of Cancer Research, Sutton, United Kingdom.

Background: For the optimal performance of high throughput genomic technologies sufficient yields of high quality DNA are crucial. Following microdissection, most samples fail to produce sufficient quantities of DNA for genome-wide experiments. Various PCR-based amplification methods have been used, but these usually produce non-uniform representations of the genome. Bacteriophage Phi29 DNA polymerase random-primed DNA amplification is based on isothermal multiple displacement amplification. We sought to define the genome representation of this method in a bacterial artificial chromosome microarray comparative genomic hybridisation (aCGH) platform.

Design: Test genomic female DNA was amplified using Phi29 amplification at 4 different starting concentrations (0.5ng, 5ng, 10ng and 50ng). These products were combined with un-amplified and amplified genomic female DNA as reference. In addition, 50 ng of DNA from 5 microdissected breast cancer frozen samples, were amplified using the same method. Three combinations were performed: un-amplified test with un-amplified reference, amplified test with un-amplified reference and both amplified tumour and reference DNA. aCGH was performed with an in-house 16K BAC platform (a resolution of ~100Kb). Pearson's correlation tests and hierarchical clustering were performed to compare the profiles obtained.

Results: aCGH profiles obtained with amplified test and un-amplified reference female genomic DNA showed copy number biases throughout the genome. These biases were more conspicuous with smaller amounts of starting material and mapped to regions with known copy number polymorphisms. When similar concentrations of test and reference DNA were amplified, the biases were cancelled out, rendering accurate profiles. For the tumours, representative profiles were obtained when both test and reference DNA were amplified.

Conclusions: Phi29 amplification preferentially amplifies specific regions mapping to known copy number variations. For accurate results using Phi29 amplification, samples subjected to aCGH analysis should be combined with reference DNA amplified with the same method, using similar amounts of starting template.

1588 Use and Validation of ERA and FOV Algorithms on Virtual Slides To Guide TMA Construction

SH Barsky, L Gentchev, AS Basu, RE Jimenez, AS Gholap. The Ohio State University College of Medicine, Columbus, OH; BioImagene, Inc, Cupertino, CA.

Background: Tissue microarrays (TMAs) are a form of high throughput screening akin to cDNA microarray and proteomic analyses, yet, unlike the latter types, are based on manual construction and interpretation. Because of the increasing demand for TMAs predicted to occur over the next decade, we felt it necessary to investigate whether their construction could be, at least partially, automated.

Design: 100 glass slides each of breast, colon and lung cancer were made into virtual slides. Image acquisition utilized scanners capable of producing images with a resolution of 20 pixels /10µ. We created both epithelial recognition algorithms (ERAs) and specific field of view (FOV) recognition algorithms that could analyze virtual slide images to select the areas richest in cancer cells. The glass slides were also used as a template to make corresponding TMAs in the traditional manner. We then compared the areas selected by our algorithms on the whole slides with the corresponding 1 mm^2 cores of the TMAs which had been manually constructed and measured their tumor cell densities (epithelial percentages).

Results: Our imaging algorithms successfully divided a virtual slide into a grid of hundreds of fields of view (FOV), each 1 mm^2, analyzed each field and identified cancer cells in a background of stroma and calculated the epithelial percentage in each field based on the ERAs. The ERAs in turn were based on applying the imaging principles of the Gaussian kernel and the elongation ratio. Those FOV with the highest epithelial percentages were mapped in terms of slide co-ordinates to be used for future TMA construction. The algorithm-based determinations were the same every time the algorithm was run on the virtual slide and therefore showed no interobserver, intraobserver or fatigue variability. Our comparative study showed that algorithm-driven selection of cancer areas were overall 25%-50% greater in cancer cell density than the cores of the TMAs which had been manually selected ($p<.001$). The overall algorithm-driven process took less than 15 minutes per slide to complete.

Conclusions: Our digital image algorithms can presently be used to guide the construction of TMAs or, in the future, to direct a robotic device to fully automate TMA production. Because of the increasing use of TMAs in both biomarker discovery and validation predicted to occur in the near future, this automation is a prerequisite for making TMAs truly high throughput.

1589 Development of a Whole Slide Image Teaching Resource for Pathology Residency Education

I Batal, M Dvorakova, M Yin, JL Fine, D Jukic, AV Parwani. University of Pittsburgh Medical Center, Pittsburgh, PA.

Background: Whole slide images (WSI) are high-resolution facsimiles of glass microscope slides that are increasingly being used in medical education, research, and anatomical pathology clinical applications. WSI are typically viewed using digital microscopysoftware that permits faculty to mark up, or annotate the image. This project represents the first stage of a large effort to comprehensively annotate the large, subspecialty teaching collections at our institute. Our overall goal was to facilitate pathology residency education in the setting of anatomic pathology subspecialty sign-out at a geographically dispersed institute.

Design: Automated whole slide image capture was performed on an Aperio T2 slide scanner (Aperio Technologies, Vista, CA) outfitted with a Nikon Plan Fluor 20x, 0.7 Numerical Aperture Objective Lens and Basler L301 "trilinear array" line scan camera. The system's spatial sampling period was approximately 0.46 microns/pixel. The system ran in automated batch mode with automated focus and tissue finding. Images were compressed during the capture process in a multi-layered JPG2000 format. The image server was equipped with dual Xeon processors, 2 GB of RAM, and 1 TB of hard drive storage running Microsoft Windows Server 2000, IIS and Aperio Image Server software version 5.6.

Results: After automated image capture, the imaging technician visually examined whole slide images for image quality. Pathologists in training viewed the whole slide images on remote workstations (located at their offices or homes) via Aperio "ImageScope". Intra-hospital connections were 100 Mbps Ethernet, and off-site connections were physically limited to consumer broadband connection speeds (typically 1.5 – 3.0 Mbps).Scan failures were caused by several factors, including tapestyle cover slips, scratched or otherwise damaged slides and/or cover slips, uneven tissue sections, and very thin sections of fatty tissue.A total of 230 interesting and representiative cases of GU pathology were created as a teaching resource.

Conclusions: WSI technology is becoming ubiquitous in educational settings but additional effort is required to fully leverage available capabilities of current WSI viewing and annotation software. A fully annotated, comprehensive collection of teaching material represents a significant investment of resources for an anatomic pathology department, particularly in settings where the number of hours devoted to resident education are diminishing due to regulatory guidelines.

1590 Evaluation of Nucleic Acid Index (NAI) in the Spectrum of Thyroid Lesions

M Begnami, M Quezado, S Wincovitch, S Garfield, MJ Merino. National Institutes of Health, Bethesda, MD.

Background: Although thyroid carcinoma is associated with abnormal nuclear DNA content, the gold standard for diagnosis remains the microscopic evaluation of H&E slides. However, crucial genomic changes may not be obvious on histologic examination. Confocal laser scanning microscopy (CLSM) has proven to improve the diagnosis of melanocytic lesions and the selection of the treatment in melanocytic neoplasias, according to the concentration of DNA and RNA in cells and represented as nucleic acid index (NAI). The purpose of our study was to calculate the NAI in thyroid lesions as a means of analyzing nucleic acid derangements in histological sections at the level of the individual cell and within the context of its microenvironment.

Design: Eight benign lesions and thirteen carcinomas representing the spectrum of thyroid lesions were evaluated. The sections were stained with acridine orange (AO), a fluorescent stain for DNA and RNA and CLSM was performed. Average fluorescent intensities of AO were measured in nuclei and the surrounding cytoplasm using Image-Pro Plus (MediaCybernetics Inc., Silver Spring, Maryland, USA) software (v5.1.2). Four to ten nuclei/cytoplasm regions were measured to determine the mean and standard deviation in each specimen. The NAI, calculated by measuring the fluorescence intensities of AO in nuclei relative to the surrounding cytoplasm, reflects the concentration of DNA relative to RNA.

Results: Papillary carcinoma showed lower NAI ratios than follicular carcinoma and benign lesions, but similar ratios to aggressive variants of thyroid cancer. Benign or malignant follicular lesions showed similar NAI values.

Conclusions: The NAI/CLSM assessment may contribute to a better understanding of morphological characteristics of thyroid lesions and may improve their diagnosis and treatment.

Nucleic acid index (NAI) in thyroid lesions

Malignant lesions	Mean ratio NAI	Benign lesions	Mean ratio NAI
Follicular carcinoma	4.36	Follicular adenoma	3.59
Follicular carcinoma	2.47	Follicular adenoma	4.69
Follicular carcinoma	3.46	Follicular adenoma	5.34
Follicular carcinoma	4.01	Follicular adenoma	4.29
Papillary carcinoma	1.97	Hurthle cell adenoma	3.26
Papillary carcinoma	1.89	Multinodular goiter	5.23
Papillary carcinoma	2.03	Multinodular goiter	3.99
Papillary carcinoma	1.65	Thyroiditis	3.83
Papillary carc,follicular variant	3.08	Total	4.27*
Papillary carc,follicular variant	2.88		
Insular carcinoma	2.18		
Anaplastic carcinoma	1.97		
Poorly differentiated carc	2.06		
TOTAL	2.61*		

*mean ratio NAI of the group

1591 Diagnostic Usefulness of Ultrasound-Guided Core Biopsy in Salivary Gland Tumours

FJ Bilbao, JL del Cura, C Ereño, R Zabala, A Fernández de Larrinoa, C Etxezarraga, JI López. Hospital de Basurto, Basque Country University (EHU/UPV), Bilbao, Bizkaia, Spain.

Background: Ultrasound-guided core biopsy (USCB) is being increasingly used in recent years in the diagnosis of superficial and deep tumour masses. However, this technique has not yet obtained a generalised acceptance among radiologists and pathologists. The reliability of USCB in the initial diagnosis of salivary gland masses has not been studied in depth.

Design: Over a 5-year period (2001-2005), a total of 38 salivary gland tumours were biopsied under ultrasound control with 18G BioPince® needles. The technique was performed in the initial approach to the diagnosis of salivary masses in the otolaryngology and head & neck consultations. Tissue fragments were submitted in cooled serum. Aside from conventional histological sections, cytologic imprints and cytocentrifugation of the transport serum were made to help in the diagnosis. Molecular analysis [IgH, TcR, and t(14;18) MBR and JH regions] was performed in selected cases of malignant lymphoma. Diagnostic correlation with surgical specimens was obtained in 14 (36.8%) cases. The clinical context and previous clinical history served as diagnostic controls in the remaining cases.

Results: Males predominated in the series (21M/16F), and the average age was 62.5 (range 27-88). Tumours arose in the parotid gland in 34 cases (89.5%) and in the submaxillary gland in 4 (10.5%). One patient had two tumours. The series included 15 primary epithelial tumours (10 mixed tumours, 4 Warthin's tumours, and 1 mucoepidermoid carcinoma, poorly differentiated), 8 lymphoid neoplasms (5 follicular lymphomas, 1 mantle-cell lymphoma, 1 MALT lymphoma, and 1 malignant lymphoma, B-cell type NOS), 3 metastatic tumours (2 squamous cell carcinomas and 1 angiosarcoma), and 7 benign lesions (4 chronic sialoadenitis, 2 lymphoepithelial lesions, 1 granulomatous inflammation, NOS, and 1 lymphangioma). The obtained material was not conclusive in 4 cases. The diagnostic accuracy was 85.7%. No major complications related to the technique were detected.

Conclusions: USCB is a useful and reliable method in the diagnosis of salivary gland tumours and should be included within the group of first-line tools in its initial management.

1592 Expression of Fascin and CD10 in Uterine Spindle Cell Tumors, a Comparative Immunohistochemical Study

AM Cano-Valdez, CB Castro Ortega, HR Dominguez-Malagon. Instituto Nacional de Cancerologia, Mexico, Distrito Federal, Mexico.

Background: Fascin is a structural protein that regulates the interaction of cytoskeleton with the cell membrane and actin fixation. It participates in migration, motility and antigen presentation by dendritic cells. Fascin expression has been explored in other tumors, but to our knowledge it has not been previously explored in uterine spindle cell tumors (USCT). The antibodies in most common use for diagnosis of these lesions include: actin, desmin and CD10, the latter has been considered useful for the diagnosis of stromal tumors. However, markers of smooth muscle tumors actin and desmin can also be positive in endometrial stromal tumors and in the stroma of mixed tumors, The aim of this work was to explore the expression of fascin in USCT, and compare it with CD10, actin, desmin and vimentin.

Design: Immunohistochemical studies for fascin, CD10, vimentin, actin, and desmin were performed in nine cases of endometrial stromal sarcomas (ESS), 20 smooth muscle tumors (SMT), and 15 endometrial mixed tumors (EMT). Comparative analysis was done to determine the sensitivity (SE) and specificity (SP) of each antibody in the three groups. The positive predictive value (PPV), and negative predictive value (NPV) of each antibody to differentiate ESS and EMT from SMT were calculated.

Results: Fascin was negative in all SMT, positive in 88% EST (SE 88.8%, SP 73%, PPV 40%, NPV 96%), and in 80% of EMT (SE 80%, SP 82% PPV 60%, NPV 90%). CD10 was expressed in 5.8% SMT, 2/6 (33.3%) of EST (SE 33.3%, SP 82%, PPV 20%, NPV 80%), and in 45% of EMT (SE 45.4%, SP 93%, PPV 62%, NPV 87). Vimentin was negative in all SMT, it was positive in 66% of EST (SE 66.6%, SP 77% PPV 37%, NPV 90%), and in (66%) of EMT (SE 66.6%, SP 86%, PPV 62%, NPV 80%). Actin was expressed in 90% of SMT (SE 90%, SP 99%, PPV 81%, NPV 95%), in 11% EST and in33% EMT. Desmin was positive in 65% of SMT (SE 65%, SP 95%, PPV 86%, NPV 89%), in 11% of EST, and in 6.6% EMT.

Conclusions: Fascin, vimentin and CD10 were constantly expressed in EST and EMT and rarely seen in SMT, the use of these antibodies is probably a useful tool for the differential diagnosis of USCT. The addition of actin provide a valuable immunohistochemical panel in the study of these lesions. Fascin was more sensible but less specific than CD10 in EST and EMT, it is less expensive than CD10 and it provides the advantage of the internal positive control in endothelial cells.

1593 Fluorescence In-Situ Hybridization Determination of Aneusomy: Criteria and Technical Considerations

BC Chadwick, C Willmore-Payne, JA Holden, LJ Layfield. University of Utah Health Sciences Center and ARUP Laboratories, Salt Lake City, UT.

Background: Fluorescence in-situ hybridization (FISH) has widespread use for evaluating gene amplification and chromosome polysomy in human maligancies. The results have both therapeutic and prognostic importance. In spite of this, definitions for chromosome polysomy vary among investigators. Many studies have not taken into consideration the proliferation index of the tumor or the thickness of the tissue specimen when using FISH.

Design: We perfomed FISH analysis to determine chromosome 7 and 13 copy number on benign normal diploid tissues (brain, colon, lymph node, tonsil) as well as on a cell line trisomic for chromosome 7 and on a cell line tetrasomic for chromosome 13. FISH analysis was done with probes recognizing the centromere of chromosome 7 (CEP7) or the centromere of chromosome 13 (CEP13). Standard 4 micron sections were studied. The proliferation index of the tissues and the cell lines was determined by immunohistochemical staining for MIB-1. MIB-1 proliferative indices were defined as the number of MIB-1 positive cells per 1000 cells counted. FISH scores were done by two different observers, each recording their results in triplicate. The FISH scores were then averaged and expressed as the mean chromosome number $\pm$ the standard deviation.

Results: Chromosome 7 FISH on normal brain, with a proliferation index of zero, ranged between 1.64 and 1.75. Diploid tissues with high proliferative indices showed chromosome 7 copy numbers greater than 2 and the counts ranged between 2.14 and 2.31. The chromosome 7 trisomic cell line showed a chromosome 7 copy number of 2.61 ± 0.23 and the chromosome 13 tetrasomic cell line showed a chromosome 13 copy number of 3.65 ± 0.16.

Conclusions: Our results indicate that FISH results are affected by the proliferation status of the tissue evaluated and by the thickness of sectioning. Low proliferative, normal dipoid tissues, have less than the expected chromosome copy number of two. This is most likely due to tissue sectioning which cuts through nuclei at various levels leaving incomplete nuclei for evaluation. The fact that some normal diploid tissues with a high proliferative index have chromosome copy numbers which overlap a trisomic cell line indicates that the definition of disomy and low polysomy should take into account cell proliferation. Our results have important implications when evaluating human malignancies for chromosome copy number by FISH.

1594 Quantitative Fluorescence-Based Analysis of Multiplexing for Immunohistochemistry

M Cregger, M Harigopal, S Siddiqui, RL Camp, DL Rimm. Yale University School of Medicine, New Haven, CT.

Background: Immunohistochemistry (IHC) allows assessment of protein expression levels without loss of spatial context. Recently, a number of groups have begun multiplexing IHC to assess multiple markers on the same slide to maximize use of scare tissue resources and/or to optimally assess the co-localization of multiple protein targets. However, multiplexing can be interpreted in many ways and has rarely been validated. Here we define 2 potential methods of multiplexing and validate each using AQUA®, a new method of in situ quantitative IHC.

Design: The common methods of multiplexing include 1) compartmental multiplexing (where antibodies are mixed and intensity is assessed on the basis of their subcellular or architectural localization), and 2) true multiplexing using multiple visualization tags on the same section. Historically multiplexing has been done with multiple enzymatic reactions (peroxidase and phophatase). Here we use only a single amplification system (peroxidase) for both methods, with intermediate HRP quenching. Each method is evaluated using a breast cancer tissue microarray with a selected set of cases and cell lines designed to optimize evaluation of estrogen receptor (ER).

Results: Her2 and ER were evaluated on a breast cancer patient cohort using both true multiplexing, and compartmental multiplexing. Linear regressions were performed to compare ER as a single marker versus true multiplexed ER showed high correlation (R=0.86). In contrast, compartmental multiplexing showed a lower correlation (R=0.66) and a scatterplot showing evidence of falsely elevated Her2 staining, presumably due to ER expression outside of the nucleus, contaminating the assessment of non-nuclear Her2. PR and p53 were used to assess the accuracy of simultaneous localization. The comparison of the multiplexed TMA with the single marker TMA shows R values for PR and p53 of 0.75 and 0.85 respectively. However, the correlation between PR and P53 is only 0.15 showing that the high correlation is not a spurious result due to common co-expression of both PR and p53.

Conclusions: While compartment multiplexing is conceivable, we show that it is inaccurate in the case of Her2 and ER. We show that that assessment in the same compartment, with HRP quenching between steps, can provide accuracy in multiplexed analysis that is comparable to that obtained when doing markers one at a time. We propose these methods as a standard for validation of multiplexing as new studies are done to optimize use of scarce tissue resources.

1595 SNP Panel Identification Assay (SPIA): A Genetic-Based Assay for the Identification of Cell Lines

F Demichelis, H Gruelich, JA Macoska, R Beroukhim, WR Sellers, L Garraway, MA Rubin. Brigham and Women's Hospital, Boston, MA; Boston, MA; Cambridge, MA; University of Michigan, Ann Arbor, MI.

Background: Tumor cell lines (CLs) are widely used in cancer research. One logistical challenge is to ensure the identity of CLs in laboratories where multiple lines are simultaneously in use or extensive cell line passaging occurs. Emerging data suggests that mixing up of CLs over time is a significant problem, which has largely gone unrecognized. High throughput SNP array studies are now finding examples of published studies using the incorrect cancer CL model. To make this more assessable to the research community, we developed and validated a SNP Panel Identification Assay (SPIA) to correctly identify tumor CLs that could be used routinely in the laboratory.

Design: To identify the ideal SNP panel, which maximizes the probability of obtaining distinct genotype calls on different samples, we used a computational multistep approach. It includes an iterative procedure of training and test steps (with bootstrap), the definition of a genotype distance and the implementation of a final statistical test, which scores a test pair as *different*, *uncertain*, or *similar*. The initial dataset included genotype data of 155 CLs derived from different organs. Genotype data of 58K SNPs were available for each CL. A subset of CLs was used for in silico independent validation. Experimental validation on a mass spectrometer system for the best panel was performed on 93 CLs.

Results: We evaluated the pair-wise distances using several sets of SNPs. The distance between 2 independent CLs increases when using a set of SNPs, sampled from the top ranked ones. On the independent validation set the mean distance increases from

0.42 (SD = 0.03) to 0.65 (SD = 0.08) for the 58K SNPs and a set of 40 selected SNPs, respectively. Similarly, the mean distance in the experimental validation set was 0.66. The statistical test scored 0 false *similar* pair and 1 true *similar* pair (MCF7 and BT20).

Conclusions: We demonstrated that the SPIA panel allows investigators to accurately identify known CLs and tumors from the genotype of extracted DNA. Although the panel is trained on the identification of CLs, this approach is suitable for additional applications, such as matching human tumor samples with their non-neoplastic normal tissue.

1596 Abstract Withdrawn

1597 Comparison of Fluorescence In Situ Hybridization (FISH) and Immunohistochemistry (IHC) for Respective *MDM2* Gene Amplification and Protein Expression in Lipomatous Neoplasms

E Downs-Kelly, J Pettay, J Weaver, S Turner, JR Goldblum, RR Tubbs. Cleveland Clinic, Cleveland, OH.

Background: The distinction of well-differentiated liposarcomas/atypical lipomatous tumors (WDLS/ALT) from benign lipomatous neoplasms can be challenging. Ring and giant chromosomes composed of 12q13-15 amplicons are identified in WDLS/ALT, which result in amplification of the *MDM2* gene. Recent publications have addressed MDM2 IHC as a tool in the diagnosis of lipomatous neoplasms. We evaluated FISH for *MDM2* gene amplification and MDM2 IHC in formalin-fixed and paraffin-embedded tissue (FFPET) as adjuncts in the diagnosis of WDLS/ALT.

Design: FISH for *MDM2* amplification and IHC for MDM2 protein was performed on FFPET whole sections from WDLS/ALT (n=14), DDLS (n=11), spindle cell/pleomorphic lipomas (SC/PL; n=6), angiolipomas (n=3), lipomas (n=3) and on a FFPET tissue microarray (TMA) containing a variety of soft tissue neoplasms. The FISH assay probes are specific for *MDM2* (12q15, Vysis®) and the centromere of 12 (*CEP12,* Vysis®). 40 nuclei/case were counted and a *MDM2/CEP12* ratio was calculated; with a ratio >2.0 considered amplified, ≤2.0 non-amplified, and ~1 with >2 signals for both probes considered polysomic for *CEP12.* Parallel IHC was performed on the Discovery XT platform using a MDM2 monoclonal antibody (Zymed, dilution 1:50) with an overall percentage of positive nuclei per case recorded.

Results: Of the WDLS/ALT, 85.7% had positive nuclei by IHC (percent positive range:5 to 30%) while all DDLS had positive nuclei (percent positive range:10-80%). By FISH, 92.9% and 100% of WDLS/ALT and DDLS showed amplification of *MDM2*, respectively (ratio:7.5). *CEP12* polysomy was noted in 5/6 (83.3%) SC/PL (ratio:0.97), all angiolipomas and lipomas were non-amplified (ratio:1) and no MDM2 expression was seen in these lesions. Of the remaining neoplasms, 1/1 epithelioid sarcoma, 1/4 malignant peripheral nerve sheath tumors (MPNST) showed *MDM2* amplification, while MDM2 protein expression was identified in the same neoplasms and in one additional MPNST. All other neoplasms were non-amplified and had no MDM2 expression.

Conclusions: *MDM2* FISH identifies amplification in atypical and cytologically bland cells within WDLS/ALT, while IHC is only positive in 5 to 30% of atypical nuclei. Therefore, the FISH assay is more sensitive than IHC in atypical lipomatous lesions, especially in limited biopsy samples. IHC may be a useful tool if FISH is not available, however one should be aware that false negatives may occur, especially on limited biopsies.

1598 Membrane-Bound Peptidase Activity in Clear Cell Renal Cell Carcinoma (CCRCC)

C Etxezarraga, A Varona, G Larrinaga, J Gil, I Hoyos, JI López. Hospital de Basurto, Basque Country University (EHU/UPV), Bilbao, Bizkaia, Spain; Faculty of Medicine and Odontology, Basque Country University (EHU/UPV), Leioa, Bizkaia, Spain; School of Nursery I, Basque Country University (EHU/UPV), Leioa, Bizkaia, Spain.

Background: Peptidases play a key role in the control of growth and differentiation of many cellular systems and are known to have a function in neoplasia. This study aims to delineate the profile of membrane-bound peptidase activity (MBP) in CCRCC.

Design: MBP activity has been investigated in a series of 45 consecutive CCRCCs. Non-tumour and neoplastic fresh tissue samples were stored at -80º in every case for enzyme assay. Sample preparation and enzyme assays were done following routine methods and protein quantification measured in units of peptidase per milligram of protein. Seven MBPs were analyzed: N aminopeptidase (APN, CD13), neutral endopeptidase (NEP, CD10), dipeptidyl peptidase IV (DPP IV, CD26), cystinyl aminopeptidase (CYS), B aminopeptidase (APB), pyoglutamyl peptidase (PG) and prolyl endopeptidase (PEP). Fuhrman's system and 2002 TNM edition were used for tumour grading and staging, respectively.

Results: Males predominated in the series (37M/8F) with an average age of 62.4 (range 37-78). Tumour diameter oscillated between 4 and 14 cm (average 7.9 cm). The tumour distribution by grade was: G2: 23 cases (51.1%), G3: 15 cases (33.3%), G4: 7 cases (15.6%). The distribution by stage was: pT1: 23 cases (51.1%), pT2: 5 cases (11.1%), pT3: 17 cases (37.6%). The table quantifies the peptidase activity showing a significant (t-Student) decrease of 5 peptidases in the neoplastic tissue.

peptidase	normal tissue	tumour tissue	significancy
APN (CD13)	36263	6273	p<0.001
NEP (CD10)	11.21	2.75	p<0.001
DPP IV (CD26)	20789	11908	p<0.01
CYS	3963	954	p<0.001
APB	11935	2225	p<0.001
PG	207	166	NS
PEP	437	439	NS

Numbers refer to units of peptidase/milligram of protein

After stratification by stage, APN activity was significantly less in pT1 than in pT2/3 (p=0.014). After stratification by grade, NEP activity was significantly less in G2 than in G3 (p=0.01) and in G2 than in G3/4 (p=0.004).

Conclusions: The activity of MBPs is significantly decreased in CCRCCs. The decrease in the activity of some peptidases is significantly different depending on tumour grade (NEP) and stage (APN). Supported by a grant from the Jesús Gangoiti-Barrera Foundation.

1599 Primary Frozen Section Diagnosis by Telepathology in Toronto: The University Health Network (UHN) Experience

AJ Evans, R Chetty, B Perez-Ordonez, S Croul, D Ghazarian, R Kiehl, B Clarke, SL Asa. University Health Network, Toronto, ON, Canada.

Background: Telepathology (TP) has been used for frozen section (FS) diagnosis in Europe and Scandinavia for over a decade. Its use for FS in North America has not been widely accepted. Concerns mainly over diagnostic accuracy have led to reluctance on the part of pathologists to learn this method of evaluating FS slides. This study describes the early experience of using TP to provide primary FS diagnoses at a major Canadian academic health science centre. This system is the first of its kind to be used for patient care in Canada.

Design: UHN comprises three sites, one of which has neurosurgery (NS) and general surgery (GS) services requiring FS support that occurs too infrequently to justify the presence of an on-site pathologist (2-5 cases/week). A dynamic TP system consisting of a robotic microscope coupled to a CCD3 camera is used to transmit 640x480 compressed JPEG images over our intranet at standard network speed (100 Mbs). The images are reviewed on monitors at the site where pathologists are located, approximately 2.5 km across the downtown of Toronto.

Results: Since November of 2004, we have used the system to make primary diagnoses on 276 frozen sections (from 203 patients), 245/276 (89%) NS and 31/276 (11%) GS. To date there has been 100% agreement between the FS and final diagnoses and no FS diagnoses have been deferred due to issues related to image quality or technical failure. The majority of cases, 155/203 (76%) have involved single pieces of tissue < 1 cm maximum dimension that could be processed without the need for gross evaluation by the pathologist and evaluated on a single frozen section slide. Turnaround times (TAT), defined from the arrival of tissue in the surgical pathology laboratory to the time the surgeon receives the FS diagnosis, have been routinely under 20 minutes. The mean time taken for the pathologists to assess the slide and communicate the diagnosis to the surgeon has been 9.98 minutes per frozen section.

Conclusions: We have found that TP is an effective and accurate means of providing primary FS diagnoses. In terms of TAT, it is our experience that this approach is ideally suited for situations where FS volumes are low and the specimens can be processed directly into FS slides by an experienced histotechnologist.

1600 Whole Slide Images Used for Immunohistochemistry Stain Interpretation in Challenging Prostate Biopsies

JL Fine, J Ho, DM Jukic, JR Gilbertson, SI Bastacky, L Anthony, R Wilson, JI Epstein, AV Parwani. University of Pittsburgh, Pittsburgh, PA; Case Western Reserve University, Cleveland, OH; Johns Hopkins University, Baltimore, MD.

Background: Whole slide images (WSI) are digital images of entire glass microscope slides. WSI based electronic distribution of immunohistochemistry (IHC) stains could permit: improved turn-around time; reduced courier costs; fewer errors in slide distribution; and automated image analysis. This report details a retrospective validation study that compared WSI and glass microscope slides for interpretation of IHC stains that were performed in difficult prostate biopsies.

Design: The study included 30 foci with IHC stains, identified by the original pathologist as both difficult and central to the final reported diagnosis. Glass slides were scanned using a T2 system (Aperio Technologies, Vista, California, USA). Data was collected from pathologists in 3 stages: 1) review of glass H&E slides; 2) review of H&E and IHC stains using WSI; and 3) review of all original glass slides. Data included individual IHC stain interpretations, overall diagnosis for each focus, and other impressions (slide/image quality; time required; diagnostic confidence). Consensus comparisons with original report diagnoses were performed, as was a separate evaluation by an expert genitourinary pathologist.

Results: Average intra-observer agreement (WSI vs glass) was 80.6% (n = 5, SD = 4.5%, range 75.7% - 86.0%). For stages 2 and 3, there was agreement by at least four pathologists in 19 of 30 foci (stage 2) and 21 of 30 foci (stage 3). Slide/image quality, time required, and diagnostic confidence showed poor inter-observer agreement. Consensus opinion was that disagreements were due to the difficult nature of the cases and not due to WSI quality limitations, and agreed with the original pathologist in 24 of 30 cases. The expert agreed with the consensus in 26 of 30 cases. Almost all such disagreements were considered reasonable in the setting of difficult cases.

Conclusions: These results are encouraging and show that WSI technology may be ready for IHC interpretation even in difficult cases. The inter-observer agreement results and consensus opinions suggest that disagreement was not due to WSI limitations. Studies that scrutinize such difficult cases serve to alert both vendors and pathologists to the limitations of this new technology, thereby stimulating future improvement.

1601 Comparative Evaluation of Three Assays for *JAK2*^{V617F} Mutation Analysis

C Frantz, D Sekora, D Henley, CK Huang, Q Pan, N Quigley, R Hubbard, I Mirza. University of Alberta, Edmonton, AB, Canada; Molecular Pathology Laboratory Network, Inc, Maryville, TN; Montefiore Medical Center, New York, NY.

Background: The recent correlation of a proportion of myeloproliferative disorders (MPD) with the *JAK2*^{V617F} activating mutation has generated a number of studies focused on characterization of the clinical features of *JAK2*^{V617F}-associated MPD as well as on the development of molecular-based assays for detection of this mutation. In this study, we comparatively evaluated three molecular methods for the detection of the *JAK2*^{V617F} mutation.

Design: A total of 36 DNA samples were analyzed by three laboratories using three methods, including an AS-PCR assay and two InvivoScribe (IVS) RFLP kit assays utilizing polyacrylamide gel or capillary electrophoresis analysis methods. Additionally, the *JAK2*^{V617F} positive samples were parallel sequenced in two of the laboratories. 35/36 samples were assayed for *BCR/ABL* by Q-PCR in the third laboratory.
Results: The study found 100% concordance among the three methods, with sensitivities of 5% for both RFLP assays and 0.01% for the AS-PCR assay. Of the 36 samples, 15 were *JAK2*^{V617F} positive, with three homozygous and 12 heterozygous positives identified by both RFLP methods. Mutation detection by sequencing proved less sensitive, with both sequencing laboratories unable to detect the mutation in differing proportions of the positive samples. Two of the 21 *JAK2*^{V617F}-negative samples were positive for *BCR/ABL*, and none of the samples assayed were positive for both *BCR/ABL* and *JAK2*^{V617F}.
Conclusions: The results indicate that the IVS kit-based RFLP assays detect the *JAK2*^{V617F} mutation with equal sensitivity regardless of analysis method, and that despite greater sensitivity of the AS-PCR method, all three methods similarly distinguished the positive and negative samples. The comparative lack of sensitivity by direct sequencing underscores the lack of advantage of this technique in *JAK2*^{V617F} mutation detection. The IVS RFLP assay kits also offer the advantages of convenience and zygosity determination, which may prove useful in monitoring disease progression or therapeutic approach.

1602 Correlation of HCV RNA in Liver and Serum of Patients with Chronic Hepatitis C

R Ghai, S Yong, U Kapur, J Ternes, S Alkan. Loyola University Medical Center, Maywood, IL.
Background: The measurement of HCV RNA levels is a vital part of management of patients with chronic HCV infection. Both quantitative and qualitative tests for HCV RNA are used to identify active infection. Viral burden for patient stratification is measured by the quantitative assay, which also provides information regarding fluctuation of viremia for modifying treatment. The relationship between serum HCV RNA levels and HCV RNA in the liver tissue is unknown. We frequently receive liver tissue for HCV testing simultaneously when there is a request for the serum assay The aim of our prospective study was to compare the results obtained by the serum quantitative HCV RNA and qualitative HCV RNA in the liver tissues in patients with history of HCV infection.
Design: A total of 126 samples of serum or liver tissue were submitted for quantitative and/or qualitative measurement of HCV RNA between Jan 2004 to Dec 2005. Clinical information was unavailable on 42 send-in samples and therefore were excluded in the final analyses. Qualitative analysis of HCV in the biopsy samples of liver tissue was performed by the ROCHE AMPLICOR HCV TEST (sensitivity: 100IU/mL). Quantitative analysis of HCV on the serum samples was performed by the COBAS AMPLICOR HCV MONITOR ASSAY (Roche Diagnostics), version 2.0 assay (sensitivity: 500IU/mL) using the HCV Quantitation standards. The genotype of HCV was determined with the LIPA assay (BAYER) using the amplicons from the ROCHE AMPLICOR HCV.
Results: Out of 84 HCV patients investigated by the molecular assays 54 patients had both serum and liver biopsy submitted for HCV analysis. In 38 patients, the HCV genotype was available (genotype 1 X 34; 2 X 1; 3 X 0; 4 X 3). There was 98.2% (53/54) concordance between the results obtained by serum and liver analysis. Only one patient tested negative by the serum assay and was positive by the qualitative liver tissue assay.
Conclusions: Our results indicate that there is significant concordance between the results obtained by the HCV RNA serum assay and the liver biopsy evaluation. There was only a single case that was detected as positive by the liver assay while the serum assay reported to be negative. This suggests that the quantitative serum assay proves to be a superior method by not only identifying the activity of the HCV infection, but also providing further information regarding the patient's ongoing therapeutic response. Molecular analysis of the liver biopsy for HCV is unlikely to provide any additional significant clinical information and therefore not recommended.

1603 Her 2/neu Status in Invasive Breast Cancers Assessed by SP3: Correlation with TAB250 and FISH

Z Ghorab, WM Hanna, HJ Kahn. University of Toronto, Toronto, ON, Canada.
Background: Her 2/neu over-expression/amplification in invasive breast cancers has been shown to be of prognostic significance as well as predictive of response to therapy. SP3 is a rabbit monoclonal antibody that reacts with the extracellular domain of human c-erbB-2(Her-2/neu oncoprotein). The aim of this study is to evaluate the expression of SP3 by immunohistochemistry (IHC) in a series of invasive breast cancers and to correlate the results with the Her2/neu status assessed by TAB 250 and by FISH.
Design: We initially assessed the Her-2/neu status using SP3 in 20 patients with invasive breast cancer with known Her-2/neu status as assessed by TAB 250 and FISH (10 were Her2/neu positive by TAB250 and FISH and 10 were negative by both markers). Subsequently IHC with SP3 and TAB 250 were assessed in additional 194 cases of invasive breast cancers. FISH analysis was performed on all IHC equivocal cases as well as 17 randomly selected positive or negative IHC cases. Equivocal for Her 2/neu oncoprotein over-expression was defined as either 2+ by IHC by either or both SP3 and TAB250 or positive reaction with only one of the two antibodies.
Results: There was 100% concordance between IHC by SP3 with TAB-250 and FISH in the initial 20 cases. Of 194 cases, 130 (67%) were negative for Her2/neu oncoprotein over-expression, 34 (18%) were positive and 30(15%) were equivocal with SP3 and TAB250. Of the 30 equivocal cases, 21 showed 2+ positivity with both SP3 and TAB250 and 9 were discordant. FISH studies on the 30 equivocal cases showed Her-2/neu gene amplification in 10 cases (7 of which were borderline or showed low level amplification) and 20 cases were not amplified.
Conclusions: There is high level of concordance between SP3 IHC and both TAB250 IHC and FISH with regard to Her2/neu assessment in invasive breast cancers. This study also indicates that FISH should be performed in equivocal cases.

1604 Immunohistochemical Comparison between New Rabbit Monoclonal Antibody (SP3) and Classical Antibodies Against HER2: Correlation with Chromogenic In Situ Hybridization in Breast Cancer Tissue Microarrays

H Gobbi, CB Nunes, RM Rocha, JS Reis-Filho, GSF Rocha, FSF Sanches, FN Oliveira. Federal University of Minas Gerais, Belo Horizonte, Minas Gerais, Brazil; Institute of Cancer Research, London, United Kingdom.
Background: Immunohistochemical (IHC) overexpression of Her2 in breast cancer is a predictive factor for response to traztuzumab. We compared a new rabbit monoclonal antibody (RabMab) with mouse monoclonal (Mab) and rabbit polyclonal antibodies using tissue microarrays (TMA) of breast carcinomas correlating the IHC results with chromogenic in situ hybridization (CISH).
Design: Sequential sections obtained from TMA containing two cores (2,0mm diameter) of 78 different breast carcinomas (total= 156 cores) were submitted to IHC using a RabMab (SP3), two rabbit polyclonal antibodies (A0485 and Herceptest - Dako) and three Mab (CB11 - Novocastra and Cell Marque, 4D5 - Genentech). Sections were also submitted to CISH (Zymed HER2 Spot-Light kit). All IHC stainings and CISH were double performed. The immunostained sections were blinded evaluated according to the Herceptest™ scoring system. CISH was evaluated according to the Zymed Her2 interpretation guide.
Results: Her2 amplification was detected in 45/78 cases (58%). The sensitivity, specificity, positive and negative predictive values (PPV and NPV) and the accuracy of the antibodies correlated to CISH are shown in table 1. Out of 39 false-positive cases, 25 (64%) were scored 2+, 9/25 (36%) were stained for SP3 and 10/25 (40%) were stained for A0485.
Conclusions: RabMab is more sensitive than other Mab, staining similar to the polyclonal antibodies A0485 and Herceptest. Most false-positive cases were scored 2+ and were stained for SP3 and A0485. Although less sensitive, both Mab (CB11 and 4D5) are more specific and more accurate than RabMab SP3 showing better correlation to CISH. Supported by FAPEMIG, CNPq, CAPES - Brazil.

Table 1 - Antibody clones, types, sources and their tests correlated to CISH

Antibody	Antibody types	Source	Sensibility	Specificity	PPV	NPV	Accuracy
SP3	Rabbit monoclonal	Labvision	100%	60%	77%	100%	83%
Herceptest	Rabbit polyclonal	Dako	97%	85%	90%	96%	92%
AO485	Rabbit polyclonal	Dako	100%	45%	70%	100%	77%
CB11	Mouse monoclonal	Novocastra	93%	97%	98%	91%	95%
CB11	Mouse monoclonal	Cell Marque	95%	97%	98%	91%	95%
4D5	Mouse monoclonal	Gennentech	97%	97%	98%	97%	97%

PPV=positive predictive value, NPV=negative predictive value

1605 Cytogenetic Analysis of Bone Marrow Samples Lacking Morphologic or Flow Cytometric Evidence of a Clonal Hematopoietic Process

AJ Goodwin, HE Fremgen, ME Tang, MR Lewis. U. of Vermont & Fletcher Allen Health Care, Burlington, VT.
Background: Bone marrow specimens are usually examined not only morphologically but also using flow cytometric and/or cytogenetic techniques. Cytogenetic results in many instances support or expand on results obtained by the other methods, but in our experience, it is unusual to find a clinically significant karyotypic abnormality in the absence of morphologic or flow cytometric evidence of a clonal hematopoietic process. We have searched for such cases in order to assess the utility of cytogenetic analysis of bone marrow samples in the absence of other abnormalities.
Design: We identified 222 cases accessioned in 2005 for which results of morphologic, flow cytometric, and conventional cytogenetic analyses of bone marrow specimens were available in our laboratory information system. Cases were categorized on the basis of (1) the presence or absence of clinically significant karyotypic abnormalities, and (2) the presence or absence of morphologic and/or flow cytometric abnormalities that fit with a clonal hematopoietic process (i.e., leukemia, lymphoma, myelodysplasia, myeloproliferative disorder).
Results: The reviewed cases were categorized as follows:

	No clonal morph or flow	Clonal morph and/or flow
Normal karyotype	74	107
Abnormal karyotype	2	39

We identified two cases in which a karyotypic abnormality was identified in the absence of morphologic or flow cytometric abnormalities. One involved a follow-up bone marrow specimen obtained from a 69-year-old man with a history of acute myeloid leukemia with t(8;21) that had initially been diagnosed nine months earlier. Despite a lack of morphologic or flow cytometric evidence of relapse, karyotyping showed t(8;21) in 3 of 20 cells, indicating cytogenetic relapse. The second case was that of an 85-year-old woman with marrow involvement by metastatic adenocarcinoma but no evidence of a clonal hematopoietic process; karyotyping showed del(X)(q24) in 2 of 20 cells.
Conclusions: We have found that clinically significant karyotypic abnormalities of the bone marrow are identified only infrequently in cases lacking morphologic or flow cytometric evidence of a clonal hematopoietic process. The two such cases identified in this series involved patients known to have malignant disease. Our findings, if confirmed on review of larger numbers of cases, would suggest that routinely completing cytogenetic analyses of bone marrow specimens that lack other evidence of a clonal hematopoietic process may be of limited clinical utility.

1606 Is Formalin-Fixed Tissue Useful for Oligo-Array CGH Studies? A Comparison with Molecular Fixative

D Gugic, M Nassiri, V Vincek, M Nadji, AR Morales. University of Miami Miller School of Medicine, Miami, FL.

Background: Array-based comparative genomic hybridization (a-CGH) is a promising tool for clinical genomic studies. The impact of pre-analytical sample preparation methods on the quality of results, however, has not been fully evaluated.

Design: Parallel sections of normal male human skin biopsy samples (n=3) were collected fresh, fixed in formalin, and in Molecular Fixative (Sakura Finetek). Genomic DNA was isolated after 8-24 hrs from the samples and subjected to amplification and labeling. Labeled samples were then co-hybridized with normal reference female DNA to Agilent oligonucleotide-based a-CGH 44k slides. Pre-analytical parameters such as DNA yield, quality of genomic DNA and labeling efficacy were evaluated. Also, microarray analytical variables, including the feature signal intensity, data distribution dynamic range, signal to noise ratio, and background intensity levels were used to assess the quality of data.

Results: The DNA yield and the quality of genomic DNA (as evaluated by spectrophotometery and gel electrophoresis) were similar in Fresh and Molecular Fixative samples. Also, the labeling efficacy of dye incorporation was comparable between the two types of samples, as were the scan parameters and stem plot analysis of a-CGH result. Formalin-fixed samples, on the other hand, showed various errors such as oversaturation, non-uniformity in replicates and decreased signal to noise ratio. In short, a-CGH results of formalin samples were not interpretable.

Conclusions: The DNA extracts of formalin-fixed material is not practical for oligonucleotide-based a-CGH studies. On the other hand, Molecular Fixative preserves tissue DNA in a manner similar to fresh state with no discernable analytical differences. Spectrophotometric and gel-based evaluation of DNA quality are not good indicators of suitability of DNA for a-CGH studies.

1607 Residency Training in Pathology Informatics: A Virtual Rotation Solution

JM Hagenkord, FA Monzon, AV Parwani. University of Pittsburgh Medical Center, Pittsburgh, PA.

Background: Pathology informatics is increasingly recognized as an important component of pathology training, and efforts are being made to provide informatics training in residency programs and also standardize the scope and objectives of this training. Traditionally, rate limiting factors in the informatics training process include: 1) many programs have limited access to pathology informatics expertise and resources, 2) a dedicated informatics rotation is difficult to carve out of an already crowded schedule, and 3) existing informatics training at one institution cannot be easily emulated by other programs due to incompatible rotation structures.We have devised a novel e-learning solution based on a resident informatics rotation at our institute which circumvents these limitations.

Design: The course is based on the instructional model designed at our institute which includes didactics given by experts in the field and hands-on laboratories. The lectures are captured as audio Powerpoints and, when feasible, laboratories are video recorded. The lectures are supplemented by readings from the textbook Practical Pathology Informatics: Demystifying Informatics for the Practicing Anatomic Pathologist by John Sinard (Springer, 2005). It is self-paced, it can accommodate various rotation structures. Module topics and depth of coverage are directed at the level of general practicing pathologist. Pre-test and post-test are based on the quizzes. Course progress, as well as completion of the pre-test, post-test, and course survey, can be tracked electronically on the website by an administrative assistant.

Results: The course is web-based and is being hosted and maintained at our institute. The course is structured as discrete modules in which the resident reads the text, views the multimedia didactics and labs, meets briefly with a local coordinator to perform a module-specific exercise, and completes an online quiz. At our institute, residents score an average of 20% correct answers on the pre-test and 70% on the post-test for an average increase after the course of 50% .

Conclusions: Experience with this material and format at UPMC has been effective in improving resident competency in pathology informatics and basic computer skills. Development of this free, web-based, self-paced, auto-graded virtual rotation in pathology informatics taught by experts overcomes many of the major limitations pathology residency programs encounter when trying to implement informatics training.

1608 Loss-of-Heterozygosity and Chromosome Copy Number Analysis in Paraffin Embedded Tissues Using Whole Genome SNP Arrays

JM Hagenkord, M Lyons-Weiler, R Dhir, A Parwani, FA Monzon. University of Pittsburgh, Pittsburgh, PA.

Background: Discrimination between benign and malignant adrenal tumors remains a conundrum for surgical pathologists. We believe that genotypic changes can be used to better assess prognosis in these tumors. Arrays for high throughput genotyping of thousands of single nucleotide polymorphisms (SNPs) have proved useful for studying gains and losses of genetic material in frozen tissues of human tumors. However, these assays don't work well with DNA obtained from formalin-fixed, paraffin-embedded (FFPE) tissues. Our goal was to develop a method for genotypic analysis of pheochromocytoma tissues from our FFPE archives with whole genome SNP arrays.

Design: DNA from frozen and FFPE samples from adrenal pheochromocytomas and paired normal tissue were processed with the Affymetrix Gene Mapping Assay with the 10K 2.0 SNP array. Samples were processed with the original manufacturer's protocol and with modifications at different steps to evaluate their effect on assay performance. Comparisons between FFPE and frozen tissue from the same tumors were performed. LOH and copy number analysis were performed using the Copy Number Analyzer for Affymetrix GeneChip mapping arrays (CNAG) software.

Results: Longer proteolytic digestion, increase in the amount of DNA, and more PCR cycles had a positive effect on SNP signal detection (SD) and call rates (CR). Frozen samples showed 99.56±0.3% SNP SD rates and 94.69±0.3% SNP CR. FFPE samples labeled with the original protocol failed to produce enough PCR product for hybridization to the arrays, while the same samples processed with the final modified protocol had SD rates of 97.35±0.018% and SNP CR of 90.85±0.034%. Agreement of SNP calls for duplicate assay samples was 99.45%±0.224% in FFPE samples and agreement between frozen and FFPE matched pairs was 95.98±1.74%. Unrelated frozen and/or FFPE samples had agreement rates of 52.76±0.84%. Using CNAG, LOH and copy number changes identified in the frozen samples were also detected in FFPE samples.

Conclusions: Our optimized protocol significantly improves the performance of FFPE samples in the Affymetrix Gene Mapping Assay with the 10K 2.0 SNP array. This optimized assay is now a valuable tool in cancer research from archived FFPE tissues. We are presently utilizing this optimized protocol to study LOH and copy number changes in archived adrenal pheochromocytomas. This will allow us to discover prognostically useful genomic differences in this morphologically homogenous group of tumors.

1609 Color Separation of IHC Stained Slides Using ImageJ, a Freely Available Software Package

A Hii, T Bloom, D Helling, KJ Bloom. CLARiENT Inc, Aliso Viejo, CA; UCLA, Los Angeles, CA; UC Santa Barbara, Santa Barbara, CA.

Background: With the emergence of targeted therapies, there is an increasing need to evaluate pathology specimens for the presence of specific protein targets. Immunohistochemistry (IHC) is a methodology for assessing the presence of proteins and coupled with image analysis may allow for quantification, since the amount of protein expressed is proportional to the optical density at a stain's specific wavelength. Unfortunately, the dyes used in routine IHC have complex overlapping absorption spectra. Three main approaches have been used to overcome this problem with limited success including attempts to define new stains with non-overlapping absorption spectra, the use of narrow-band filters to selectively measure only the spectra at a dye-specific wavelength and the use of color transformation techniques. ImageJ is a freeware program based on NIH image. Ruifrok et al developed a color deconvolution plugin for ImageJ that purports to separate individual colors even when stains are colocalized. The purpose of this study was to optimize this color deconvolution algorithm to allow easy separation of hematoxylin and DAB allowing for the accurate assessment of quantitative nuclear stains such as ER.

Design: Fifty images were acquired from a breast carcinoma tissue microarray, created at CLARiENT Inc. and stained for ER using the PharmDx kit (Dako). Images were acquired as jpegs using the MedMicro software package, (Trestle) and were then analyzed using ImageJ (rsb.info.nih.gov/ij). The color deconvolution algorithm was obtained from http://www.dentistry.bham.ac.uk/landinig/software/software.html. The matrix settings were systematically altered to optimize the separation of the original image into two daughter images, one containing only unstained nuclei and the other containing only stained nuclei.

Results: The original matrix settings in the downloaded algorithm 0.650, 0.704 and 0.286, created an acceptable daughter image for the unstained nuclei; but they were unacceptable for the stained nuclei, those expressing DAB. Through trial and error, matrix settings of 0.15, 0.95, 0.15 created the best daughter images, in which only the positive staining nuclei were represented. These settings created appropriate daughter images from all 50 jpeg images.

Conclusions: It is possible to use freely available image analysis software to segment standard IHC stained images into daughter images that can then be easily classified and enumerated.

1610 An Algorithm for Counting IHC Stained Nuclei Using ImageJ, a Free Image Analysis Software Package

A Hii, T Bloom, D Helling, KJ Bloom. CLARiENT Inc, Aliso Viejo, CA; UCLA, Los Angeles, CA; UC Santa Barbara, Santa Barbara, CA.

Background: Quantification of nuclear proteins by immunohistochemistry provides important prognostic information in a variety of carcinomas. Several commercial image analysis programs are available but most use pixel based counting algorithms that suffer from a variety of problems, the most important of which is the inability to gate tumor cells since pixel based methods do not see objects. Object identification and classification is a complex problem, but if solved would provide pathologists with a reproducible way to quantify the proportion of tumor cells showing nuclear expression of a protein.

Design: Fifty images were acquired from a breast carcinoma tissue microarray, created at CLARiENT Inc. and stained for ER using the PharmDx kit (Dako). Images were acquired as jpegs using the MedMicro software package, (Trestle) and were then analyzed using ImageJ (rsb.info.nih.gov/ij). Each image was subject to color deconvolution creating two daughter images, one containing only negative nuclei and one containing only only positive nuclei. Each image was then subjected to the same binary manipulation consisting of executing 3 sharpen, 1 threshold, 1 erode, 1 dilate and 1 watershed algorithm. Each image was then counted using the analyze particle function built in to ImageJ, setting the minimum particle size to 10 pixels and compared to the manual counting of the same images. Scores were binned using the proportional score of the Allred scoring system which places the percentage of stained nuclei into 6 bins: 0%, 0-1%, 1-10%, 10-33%, 34-66% and 67-100%.

Results: Thirty-seven (74%) of the fifty images were categorized correctly by the algorithm. The remaining 13 cases were off by at most 1 category. See table for complete results.

Conclusions: Object identification and classification is possible using freely available image analysis software. Although further enhancements to the algorithm is necessary before clinical deployment, the basic functionality is in place.

Proportion Score - Manual (x-axis) vs Computer assisted (y-axis)

	0%	0-1%	1-10%	10-33%	34-66%	67-100%
0%	10	0	0	0	0	0
0-1%	0	0	0	0	0	0
1-10%	0	0	2	1	0	0
10-33%	0	0	1	1	1	0
34-66%	0	0	0	2	8	7
67%-100%	0	0	0	0	1	16

1611 Integration of Whole Slide Images into Anatomic Pathology Workflow

J Ho, DM Jukic, JL Fine, A Parwani, JR Gilbertson. Universty of Pittsburgh Medical Center, Pittsburgh, PA; Case Western Reserve University, Cleveland, OH.

Background: Adoption of whole slide image (WSI) technology has largely occurred primarily in the pre-clinical (research) and peri-clinical (educational) spaces, and adoption in the clinical space is presumed to be rapidly approaching.However, large scale clincal application of whole slide images into anatomic pathology workflow will require communication between whole slide image systems and existing hospital infrastructure, including the anatomica pathology laboratory information systam (APLIS), picture archiving and communications system (PACS), and patient registration. We integrated a commercial automated imaging device, and then created and evaluated a prototype integration system. Finally we provided feedback to the industry for broader acceptance, development, and growth of WSI.

Design: The prototype consisted of a middleware application that interfaced with the LIS, the imaging device, security servers, and the pathologist. Key characteristics of the application included messaging capabilitiy between the imaging devices and the LIS (matching patients, accessions, and slides), the ability to create and transfer WSI to an independent archive, and a novel interface that allowed pathologists to examine whole slide images in the contect of the patient and the case.

Results: The prototype system was able to facilitate the incorporation of WSI into the anatomic pathologist's workflow by managing (1) the acquisition of WSI into enterprise storage, (2) the association of WSI with the patient and specimen, and (3) the presentation of the WSI in the context of the case and clinical picture.

Conclusions: Data integration between the LIS and imaging devices - through bar coded slides and middleware - seems to be important in large scale clinical use of WSI. The LIS should remain the major workflow engine of pathology, and clinically effective systems should present textual and image data on the same user interface. Furthermore, a workflow-centric interface may be helpful in optimizing the diagnostic/clinical examination of whole slide images.

1612 The Effect of Histological Tissue Sample Size on the Sampling Error

V Iakovlev, M Pintilie, A Morrison, A Fyles, R Hill, D Hedley. University Health Network, University of Toronto, Toronto, ON, Canada; CIHR, Toronto, Canada.

Background: A fundamental principle of the sampling theory is the inverse relationship between the analyzed sample size and the sampling error. Distributional and constitutional heterogeneity of the molecular markers are frequently overlooked in study designs; this may lead to a large sampling error and ultimately inconclusive results.

Design: pO2 measurements by the Eppendorf electrode and multiple biopsies were taken from cervical carcinomas of 24 patients. The biopsies were sectioned at multiple levels, stained for the surrogate hypoxia marker Carbonic Anhydrase IX (CAIX) and analyzed by semi-automated, high accuracy image analysis approaches. Tissue microarrays were simulated to test the suitability of this technology for CAIX quantification. A 3D restoration was generated to visualize the spatial arrangement of CAIX distribution. Models of staining were designed to demonstrate the relationship between the biopsy size and the sizes of the positive foci.

Results: More than 40% of the tumors could not be categorized with 95% confidence at the critical CAIX% cut-offs, due to the extent of CAIX variability. Biopsy size and the cumulative volume of the tissue sample were the major factors affecting the degree of this variability. There was a weak correlation of CAIX with the pO2 measurements. The tissue microarray simulations showed an inverse relationship between the sampling error and the number of spots and their diameters.

Conclusions: The data demonstrate the importance of preliminary assessment of the required tissue sample size, in order to reduce the sampling error to a desired level. The size of the foci of positivity and the average percentage of expression are needed in order to calculate the sampling error for a given sample size. We demonstrate this adapting the sampling theory to histological samples.

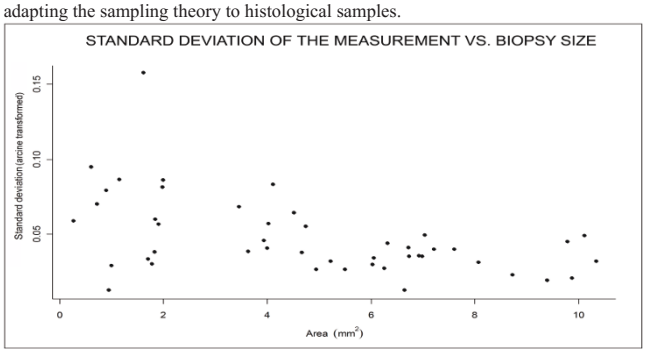

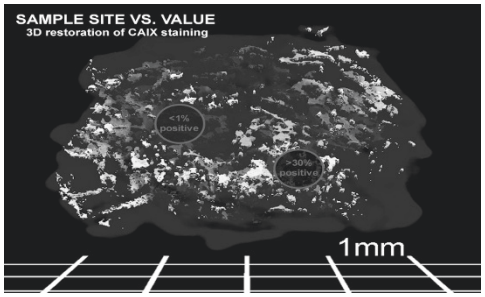

1613 Validation of a 10 Gene Multiplex Quantitative Reverse Transcriptase-Polymerase Chain Reaction (qRT-PCR) Assay To Detect the Primary Site of Metastatic Carcinoma of Unknown Origin (CUP)

CK Ibrahim, J Baden, C Major, A Mazumder, K Gray, CE Sheehan, B Varadarajalu, MS Ross, DM Jones, T Nazeer, TA Jennings, JS Ross. Albany Medical College, Albany, NY; Veridex, LLC, Warren, NJ.

Background: Despite advances in biomedical imaging and minimally invasive surgical techniques, the determination of the primary site in CUPs remains a challenge in clinical practice. There has been significant interest in the use of molecular techniques to complement traditional morphology in the assessment of these metastatic lesions.

Design: Using transcriptional profiling, literature searches and a quantitative RT-PCR technique (Veridex, LLC), a 10 gene classifier was developed on 205 formalin fixed paraffin embedded (ffpe) CUPs to predict the primary site of origin. The RT-PCR assay detects primary tumor sites as: breast, colon, small and non-small cell lung, ovary, prostate, pancreas and "other." The 10 gene classifier was subsequently tested on 48 CUPs not included in the discovery set. In the current study, the 10 gene classifier was validated on an additional 10 CUPs whose site or origin was assessed by immunohistochemistry (IHC) and confirmed by follow-up clinical studies.

Results: The qRT-PCR technique featured an initial one-out cross validation accuracy of 78% and a 76% accuracy with the initial test set. The primary sites for the 10 case new validation set were lung (3), colon (3), gallbladder (1), endometrium (1), head and neck (1) and ovary (1). The qRT-PCR assay correctly identified the primary tumor site in 8 (80%) of the cases. The endometrial and head and neck primary tumors were classified as "other" by the qRT-PCR assay. The decision algorithm prediction averaged 83% (range 37% to 100%). In one case of poorly differentiated metastatic gallbladder cancer, the qRT-PCR assay predicted a small cell lung cancer origin while the IHC was not conclusive. In another case of metastatic adenocarcinoma with enteric features originating in the lung, the qRT-PCR assay predicted colorectal rather than pulmonary origin. IHC classification was not conclusive in this case with negative stains for both cytokeratin 20 and TTF-1.

Conclusions: The 10 gene multiplex qRT-PCR assay designed to identify the primary tumor site in cases of CUP had a high accuracy of 80% in this validation study using ffpe tissues. Further evaluation of this qRT-PCR technique on larger cohorts of patients is warranted to confirm the high accuracy and the potential clinical utility of the technique.

1614 Sentinel Lymph Node Evaluation: The Cutting Edge

JA Jarzembowski, KN Altmann. Washington University in St. Louis, St. Louis, MO; Elon University, Elon, NC.

Background: Sentinel lymph node evaluation represents an integral part of staging skin and solid organ malignancies for optimal treatment and prognosis, but most protocols have no standardized procedure for gross lymph node processing. Current practices vary with surgeon preference, pathologist preference, and institutional tradition. Published studies have improved lymph node evaluation by cutting multiple tissue sections and/or using immunohistochemistry, but few studies have ascertained the optimal gross preparation of lymph nodes for metastatic detection. The ideal grossing method would produce maximal surface and subcapsular areas because metastases are more commonly found in the subcapsular and hilar regions.

Design: We mathematically modelled a lymph node as an ellipsoid. Variables included nodal dimensions (long and short axes, 0 to 4 cm), sectioning direction (parallel or perpendicular to the long axis), and section thickness (0.5, 1.0, or 2.0 mm). We also compared serial sectioning of the node versus serial bisection versus initially bisecting through the hilum and then making subsequent sagittal cuts. Because the resulting equations could not be solved explicitly, we used graphical analysis to determine trends over a range of sizes corresponding to anatomically relevant nodal dimensions (< 3 cm). We then randomly placed variously sized metastatic foci (0.2 - 2.0 mm) in either parenchymal or subcapsular locations and determined the detection rates for each cutting method. Results were based on 100,000 simulated metastases per method.

Results: Sectioning lymph nodes parallel to the longitudinal axis generally yields greater evaluable parenchymal area and subcapsular area compared to perpendicular sectioning, and does so in fewer tissue pieces. In the most extreme circumstances, the cutting methods differ in total area by 2-fold and in subcapsular area by 1.5-fold. The method of longitudinal bisectioning has a higher theoretical metastatic detection rate (up to 200% higher), regardless of tumor location, than all other cutting protocols ($P < 0.003$).

Conclusions: Lymph nodes should be cut, as thinly as possible, parallel to their long axis by first bisecting through the hilum, then sequentially bisecting the remaining pieces with outward sagittal cuts. Doing so generally maximizes the total and subcapsular areas represented on the slides but most importantly finds more metastases. Using this gross preparation method may increase the metastatic detection rate, both by routine microscopy and by immunohistochemical stains.

1615 Diagnostic Capability Depends upon the Type and Volume of the Transport Media: A Study of 214 Fine Needle Aspirates from Deep Seated Organs

NC Jhala, J Webster, IA Eltoum, DR Crowe, DC Chhieng, DN Jhala. University of Alabama at Birmingham, Birmingham, AL.

Background: Fine needle aspiration (FNA), especially endosonography (EUS) guided has rapidly gained prominence as a method of choice for obtaining diagnosis for deep seated lesions. Often times cells obtained using this modality is scant and requires ancillary studies to arrive at definitive interpretations. Each laboratory uses some transport media such as Cytolyt or Hanks balanced salt solution (HBSS) to process their samples to perform diagnostic tests. This study is conducted to determine if the type and volume of transport media can improve diagnostic performance of providing diagnosis on EUS-FNA samples.

Design: A total of 214 consecutive EUS-FNA cases were evaluated from pancreas (n= 99), lymph node (n=73), and other sites (n= 42). These patients ranged from 15- 91 years. For each case smears were evaluated and at least one additional pass was either collected in 30 c.c. Cytolyt, 10 c.c. HBSS or 5 c.c. HBSS and paraffin embedded cell blocks were prepared. H&E sections were evaluated to assess the cellularity and perform immunohistochemical stains to arrive at definitive diagnosis. Immunophenotyping studies were requested using flow cytometry when a lymphoma was suspected.

Results: The frequency distribution for our diagnoses included: positive for malignancy (n=102), atypical/suspicious for malignancy (n=24), reactive (n=32), and non-diagnostic (n=56). Cell blocks could be prepared in 108 of 214 (50.4%) cases. It was noted only HBSS but not cytolyt could be used to perform immunophenotyping on FNA suspected of lymphoma. The cell count in these samples ranged from 30,000 – 3.4 million. Volume did not affect cellularity or ability to perform immunophenotpying. Cell blocks with adequate cellularity were obtained significantly ($p = 0.025$) more frequently when samples were transported in 5 c.c. HBSS 83% (34/41) in comparison to either 10 CC. HBSS 59% (37/63) or Cytolyt 4.5% (4/88). In 38% of cases performance of ancillary studies on cell blocks helped to arrive at accurate diagnosis including characterizing the cell type.

Conclusions: Low volume HBSS should be utilized as a transport medium to collect samples obtained from EUS-FNA to obtain more informative samples.

1616 Morphology-Based Molecular Diagnosis for Targeted Cancer Therapy Using Formalin-Fixed Paraffin Embedded (FFPE) Sections

H Kajiya, A Serizawa, H Itoh, T Minematsu, T Susumu, RY Osamura. Tokai University School of Medicine, Isehara, Kanagawa, Japan.

Background: Recently, both advanced and early cancers have been treated with the molecular targeted therapy which are mainly performed by humanized monoclonal antibodies or tyrosine kinase inhibitors. The most efficient treatment is expected in the tumors by the appropriate detection of targeted gene expressions, such as DNA mutations and specific mRNA expressions as well as FISH or CISH. We hereby describe the morphology-based techniques to perform molecular diagnosis, i.e. PCR and RT-PCR, using the selected tumor areas on the FFPE sections.

Design: The tissues were fixed by 10% formalin and embedded in paraffin. 4mm sections were attached to glass slides. These tissue sections were subjected to PCR and RT-PCR, by scraping sections or by selecting specific areas by laser capture microdissection (LCM: Arcturus). Detection of DNA mutations of genes such as c-kit in gastrointestinal stromal tumor (GIST) and, RET in medullary thyroid carcinomas (MTCs) and the detection of particular somatostatin receptor (SSTR)2 mRNA in pancreatic neuroendocrine carcinoma (NEC) were successfully performed. For DNA extraction, deparaffinized tissues were incubated overnight with proteinase K, and then DNA extraction was performed using a phenol + chloroform solution. PCR products were subjected to automated sequencing for the human c-kit and RET gene mutation analysis. For total RNA, deparaffinzed sections were extracted using TriZol reagent and RT was performed using StrataScript. And RT-PCR of SSTR2a was performed.

Results: In the GIST, the DNA extracted from FFPE sections by LCM showed recognizable bands and subsequent DNA sequencing showed deletion of 28aa-33aa of exon11 in c-kit gene and the tumor was expected to be responsive to Imatinib therapy. DNA extracted from the MTC of a case of de novo MEN2b showed a somatic point mutation at codon 918 which reportedly predicts the worse prognosis and suggests possible use of tyrosine kinase inhibitors.RT-PCR detected single band of SSTR2a from the FFPE sections of pancreatic NEC with hepatic metastasis. This patient received the somatostatin analoque (Octreotide) therapy and the metastatic disease responded.

Conclusions: The techniques for successful detection of DNA mutation and specific mRNA from the archival FFPE sections are particularly important for the appropriate patient care in practice of surgical pathology.

1617 Fluorescence In Situ Hybridization Using Core Needle Biopsies on Paraffin-Embedded Brain Tissue for Detection of 1p36 and 19q13 Deletions

B Khandpur, I Ahmad, C Bryant, J Delayo, R Siddiqui. Danbury Hospital, Danbury, CT.

Background: Diffuse gliomas are the most common primary CNS malignancies. Oligodendrogliomas and other low-grade gliomas are associated with chromosome 1 and chromosome 19 abnormalities and have a long survival rate and good therapeutic response to chemotherapy. To date, there are no reliable histopathological criteria to differentiate these lesions. Additional diagnostic tools are needed to facilitate the diagnosis and treatment of these lesions in a timely manner.

Design: Identifying deletions in chromosomes 1p and 19q will help in predicting a favorable prognosis and potential response to chemotherapy. Fluorescence in situ hybridization (FISH) has the best ability to detect these alterations when these are present in as few as 20- 30% of the cells. FISH can be performed on thin sections from paraffin embedded blocks but this method is limited because of truncation of cell nuclei being studied due to necessity of splicing through the tissue. The aim of our study was to explore an alternative procedure for processing paraffin embedded tissues to study gliomas using FISH. Needle core biopsies were obtained from paraffin embedded tissue blocks using a blunted, 21 gauge needle. Biopsies were taken from 13 brain tumor specimens. Autopsy brain specimens were used as normal controls. These biopsies were then deparaffinized, rehydrated, digested and fixed. The resulting cell suspension was placed onto slides and a FISH assay, using commercially available probes for 1p36 and 19q13, was performed on each specimen. Intact nuclei were obtained from all the samples.

Results: Adequate FISH results were achieved in 13/14 specimens. Hybridization was successful for chromosome 1p probe in thirteen (13/14) cases and for chromosome 19q in all cases (14/14). 19q13 deletion was detected in 2/14 cases.

Conclusions: FISH results from thin sections of paraffin embedded tissue may be difficult to interpret due to inherent truncation of nuclei. For informative FISH studies, needle core biopsy technique appears to be an effective method of obtaining intact nuclei from paraffin embedded tissue.

1618 Interphase FISH Analysis of Paraffin-Embedded Tissue Microarrays Is a Rapid, Sensitive, Specific and Cost-Effective Method for Identifying Specific Chromosomal Translocations

ME Law, A Dogan, ED Remstein. Mayo Clinic, Rochester, MN.

Background: Several recurrent balanced translocations have been identified in extranodal marginal zone B-cell lymphoma of mucosa-associated lymphoid tissue (MALT lymphoma). These translocations, including *API2-MALT1*, *IGH-MALT1, IGH-BCL10,* and *IGH-FOXP1,* all involve *MALT1* and/or *IGH,* and together are present in about 25% of MALT lymphomas. Detection of these translocations is important for both diagnostic and prognostic purposes. Although interphase fluorescence in situ hybridization (FISH) performed on nuclei isolated from paraffin-embedded tissue cores effectively detects specific chromosomal abnormalities, it is a very labor intensive, expensive and time consuming technique. Here, we compared the utility of interphase FISH performed on thin sections of paraffin-embedded tissue microarrays (TMA) versus isolated nuclei in screening for common translocations in MALT lymphoma.

Design: Five micron sections of TMAs composed of paraffin-embedded cores from 108 MALT lymphomas from a variety of anatomic sites and 7 normal tonsils were studied by FISH using breakapart (BAP) probes for MALT1 and IGH. Isolated nuclei from paraffin-embedded cores from all 115 specimens had been previously studied by FISH using BAP probes for MALT1 and IGH.

Results: A FISH result was not produced in 10/115 and 13/115 TMA specimens using the MALT1 and IGH FISH probes, respectively, while all 115 isolated nuclei specimens were successful using both probes after one or more attempts. The FISH results using the MALT1 BAP and IGH BAP probes on the successful specimens are listed in Tables 1 and 2 below.

MALT1 FISH: TMA vs Isolated Nuclei (Gold Standard)

True Positive: 30	False Negative: 0
False Positive: 0	True Negative: 75

IGH FISH: TMA vs Isolated Nuclei (Gold Standard)

True Positive: 9	False Negative: 0
False Positive: 0	True Negative: 93

Conclusions: Interphase FISH performed on thin sections of paraffin-embedded TMAs is a very useful method for screening for specific chromosomal translocations in MALT lymphoma, showing a 90% success rate and 100% specificity and sensitivity compared to the gold standard of isolated nuclei from paraffin embedded tissue. It is more cost-efficient, requiring less tissue, less FISH probe, and less time for sample preparation and interpretation. This technique will likely be applicable to detection of other specific chromosomal abnormalities in sets of other types of neoplastic specimens.

1619 Extraction and Amplification Methods To Enhance Expression Analysis from Formalin Fixed Paraffin Embedded (FFPE) Tissues

J Li, P Smyth, S Cahill, K Denning, R Flavin, S Guenther, J O'Leary, O Sheils. Institute of Molecular Medicine, St James's Hospital, Dublin, Ireland; Applied Biosystems, Foster City, CA.

Background: Archival formalin-fixed paraffin-embedded (FFPE) tissues represent an abundant source of clinical specimens, however their use is limited in applications involving analysis of gene expression due to RNA degradation and modification during fixation and processing. This study examined a panel of four commercially available extraction kits in conjunction with in-house modification to recommended protocols. Further, it evaluated a novel pre amplification system designed to enhance expression analysis from tissue samples.

Design: N-thy-ori cells were grown to confluence and aliquots with equal cell numbers were (a) snap frozen and (b) formalin fixed and paraffin embedded into a cell block. RNA was extracted in parallel using selected protocols: Stratagene Absolutely RNA FFPE Kit, Gentra Purescript RNA Purification Kit, Ambion RecoverAll Total Nucleic Acid Isolation Kit, and Invitrogen Trizol Reagent (according to manufacturer's protocols), in addition to modified Stratagene and Ambion protocols. The quality and quantity of RNA yields was measured with Bioanalyzer, Nanodrop and TaqMan® assays with and without pre-amplification using a panel of assays with a range of amplicon size (71-124 bp).

Results: The results from Bioanalyzer and TaqMan® showed variations in RNA quality dependant on the protocol used. On FFPE extracts - Stratagene and Ambion kits gave superior results than the others examined. Modification to Stratagene and Ambion protocols generated still better results. TaqMan® analysis with pre-amplification consistently achieved decreased C_T values in both snap frozen and FFPE aliquots compared with no pre-amplification. Using CDNK1 as the endogenous control, $\Delta\Delta C_T$ results were consistently between –2 and + 2 provided assays and endogenous controls were matched with regard to approximate amplicon size.

Conclusions: Evaluation of a series of RNA extraction kits has identified protocols, which reproducibly produce RNA that may be successfully amplified using Q-RT-PCR. TaqMan® pre-amplification system is a robust and practical solution to limited quantities of RNA from FFPE extracts.

1620 Automated In Situ Hybridization and Immunohistochemistry for Cytomegalovirus Detection in Paraffin-Embedded Tissue Sections

DY Lu, SM Waldrop, C Cohen. Emory University, Atlanta, GA.

Background: Cytomegalovirus (CMV) infections are a major cause of morbidity and mortality in neonates and immunocompromised individuals (organ transplant recipients, patients receiving chemotherapy/immunosuppressive drugs, HIV-infected individuals). The most common manifestations of CMV disease are pneumonia, retinitis, and gastrointestinal disease. CMV detection methods include CMV antibody testing, viral culture of urine and tissue samples, polymerase chain reaction (PCR) of blood, and histology of tissue samples. In situ hybridization (ISH) and immunohistochemical (IHC) techniques prove to be more sensitive than routine hematoxylin-eosin (H&E)-stained slides. Until recently, ISH was performed manually. We compared CMV results of automated ISH and IHC techniques in previously diagnosed CMV-infected tissues.

Design: Seventy-two previously studied cases for CMV (44 gastrointestinal tract, 4 livers, 1 spleen, 19 lungs, 2 brains, 1 placenta, 1 kidney) were re-evaluated using automated ISH and IHC methods. Of the 72 cases, 36 were originally diagnosed as CMV-positive, 28 CMV-negative, and 8 CMV-equivocal. Original diagnoses were rendered on H&E sections, by automated IHC, manual ISH, PCR, and/or viral culture. With the Bond-max autostainer (Vision BioSystems), automated ISH and IHC techniques were performed, using prediluted CMV probe and NCL-CMVpp65 monoclonal antibody (1:500 dilution) (Novocastra), respectively.

Results: By automated ISH, 27 cases were CMV-positive (25 positive, 2 equivocal on original diagnosis), 43 were negative (9 positive, 28 negative, 6 equivocal on original diagnosis), and 2 were equivocal (both positive on original diagnosis). By automated IHC, 31 cases were CMV-positive (28 positive, 3 equivocal on original diagnosis), 39 were negative (6 positive, 28 negative, 5 equivocal on original diagnosis), and 2 were equivocal (both positive on original diagnosis). Using the original CMV diagnosis as gold standard, automated ISH and IHC had a sensitivity of 69% and 78%, respectively, and a specificity of 66% and 75%, respectively. Automated ISH and IHC correlated significantly with each other ($p < 0.01$) and with the original diagnosis ($p < 0.01$).

Conclusions: Both automated ISH and IHC are recommended for CMV detection in paraffin-embedded tissue samples. They have similar sensitivity and specificity. They are easy to perform, requiring only set-up technologist time. Interpretation is aided by strong stain intensity and lack of background.

1621 RNA Yields and RT-PCR Gene Expression Profiles Obtained from Manual-Microdissected, Fixed-Paraffin-Embedded Tissue (FPET) from Prostate Adenocarcinomas

C Magi-Galluzzi, F Baehner, D Dutta, T Maddala, D Watson, JW Cowens, E Klein. Cleveland Clinic, Cleveland, OH; Genomic Health, Redwood City, CA; University of California, San Francisco, CA.

Background: From prostatic adenocarcinomas we examined the RNA extraction yields and gene expression profiles obtained from whole section (WT), enriched tumor tissue (ET) and non tumor tissue (NT) using a RT-PCR assay designed to quantitate the small fragments of RNA present in FPET. Here we report the differential RNA yields and gene expression profiles obtained from ET, NT and WT.

Design: FPET blocks from 10 radical prostatectomy specimens in patients without metastatic or Stage IV disease were used. Three 10 µm unstained FPET WT sections or six 10 µm unstained FPET manual-microdissected ET and NT sections were separately analyzed. Extracted RNA yields and the expression levels of 380 cancer-related genes and 4 reference genes were measured from WT, ET and NT using RT-PCR in a 384 well format on the ABI 7900HT real time PCR instrument. Expression for each gene was normalized relative to reference genes. Differences in gene expression from ET and WT, ET and NT, and NT and WT were calculated and paired sample t-tests were used to identify differences in gene expression.

Results: The RNA yield per unit surface area in ET compared to NT was approximately three fold higher (average RNA yield of 61.0 ng/mm^2 for ET compared to 20.8 ng/mm^2 for NT). Differential gene expression was observed among ET, NT, and WT. Eighty genes were more highly expressed in NT compared to ET tissues (unadjusted p-values <0.05) and 45 genes were more highly expressed in ET compared to NT tissues (unadjusted p-values <0.05). With 384 genes being evaluated the expected number of false discoveries was 19. A number of potentially important prostate cancer biomarkers were highly differentially expressed in ET versus NT (e.g., AMACR1 & ALCAM higher in ET; IL6 & CDKN1A higher in NT).

Conclusions: ET contains higher RNA yields per unit surface area than NT or WT. Differential gene expression is evident among ET, NT, and WT. Optimal quantification of candidate biomarker gene expression in prostate adenocarcinomas will require manual microdissection.

1622 Immunohistochemical Evaluation of Expression and Distribution Pattern of Novel Vascular Markers (CD105 and D2-40) in Cirrhosis and Hepatocellular Carcinoma

RK Malhotra, W Li, PT Cagle, D Tan. UT-Houston, Medical School, Houston, TX; The Methodist Hospital, Hosuton, TX; MD Anderson Cancer Centre, Houston, TX.

Background: CD105 and D2-40 are two novel proteins expressed by neoplastic vasculature. Though they have been recently tested in several human malignancies, their expression and distribution pattern in hepatocellular carcinoma(HCC), a highly vascular tumor, has been little studied. This study tested the working conditions and distribution patterns of CD105 and D2-40 in cirrhotic liver and HCC.

Design: Immunohistochemistry was performed for the expression of CD105 and D2-40 in HCC from 51 consecutive patients. Thirty-nine HCCs also contained background cirrhosis. To maximize the working conditions and ensure quality methodologies, different combinations of antigen retrieval, biotin blocking and peroxidase deactivation were tested, along with paralleled immunohistochemistry of established vascular markers like CD31 and CD34.

Results: The characteristics of CD105 and D2-40 used in this study, and their detecting conditions are summarized in Table 1. Diffuse expression of CD105 was noted in 32 cirrhotic liver specimens, with sinusoidal pattern and stellate branches. 24 HCCs displayed immunoreactivity with CD105, 6 of which were focal. In contrast to cirrhotic counterparts, HCCs showed an encircling pattern of CD105 positive endothelial cells around malignant hepatocytes. The endothelial cells in both cirrhotic and HCC components revealed little, if any, D2-40 immunoreactivity. However, vascular spaces in the fibrotic portal septa were strongly positively of D2-40. CD31 and CD34 frequently showed delicate staining in the endothelial cells of HCCs as well as, to a lesser extent of endothelial cells in cirrhotic sinusoids.

Conclusions: Characteristic sinusoidal expression pattern of CD105 in cirrhotic liver and encirclement pattern of CD105 in HCC may offer added value in differential diagnosis of these two entities, particularly in biopsy and cytology specimens. The significance of differential expression of D2-40 in reactive (fibrosis) and neoplastic liver warrants further investigation.

Table 1: Characteristics and methodologies of CD105 and D2-40

Marker	Vendor	Catalog#	Pretreatment	Detection	Peroxidase blocking	Chromogen
CD105	Dako	M3527	Proteinase K 5min	CSA(K1500)	5min	DAB
D2-40	Signet	730-01	T.9 30min	CSA(K1500)	10min	DAB

1623 15-Minute Detection of a Prostate Cancer Biomarker (AMACR) in Voided Urine Samples Using Immuno-Cantilever Sensors

D Maraldo, FU Garcia, R Mutharasan. Drexel University, Philadelphia, PA; Drexel University College of Medicine, Philadelphia, PA.

Background: Prostate cancer (PCa) detection needs more sensitive and specific tools. We developed a novel urinary test for prostate cancer that detects α -methylacyl-coA racemase (AMACR) in voided urine. The test utilizes a piezoelectric-excited millimeter-sized immuno-sensors (PEMC) that have mass change sensitivity of femtograms and a 15-minute measurement time.

Design: Clean catch voided urine specimens of were prospectively collected on five patients with confirmed prostate cancer 3 weeks after prostate biopsy. The mean age of the patients was 65 . The presence of AMACR was evaluated in a blinded manner by exposing 3 mL of urine to PEMC sensor with immobilized anti-AMACR. PEMC sensor frequency response data was collected and compared with control urines.

Results:

Case #	Age	Gleason Score	Post Biopsy Stage	PSA Value	PEMC Value	PEMC Control Urine
Case 1	61	7	pT2c	11.6 ng/ml	4,314±35 Hz	10±21 Hz
Case 2	83	6	pT2a	12.6 ng/ml	259±14Hz	10±6 Hz
Case 3	64	8	pT2c	78.4 ng/ml	935±80Hz	-63±14 Hz
Case 4	59	7	pT2b	4.6 ng/ml	600±31 Hz	-35±24 Hz
Case 5	65	7	pT2c	2.0 ng/ml	801±81 Hz	-20±15 Hz

Conclusions: We report a rapid non-invasive test to detect Pca in voided urine. PEMC sensors detected the presence of AMACR in voided urine within 15 minutes in confirmed Pca patients. This test maybe a useful adjunt in the outpatient setting to identify men at increased risk for prostate cancer.

1624 Pathology Informatics Tools To Support Translational Research

SK Mohanty, AA Patel, AV Parwani, MJ Becich. University of Pittsburgh, Pittsburgh, PA; University of Pitsburgh School of Medicine, Pittsburgh, PA.

Background: Recent advances in genomics, proteomics, and clinical trials have transformed the landscape of cancer research, fueling the development of translational research programs that connect clinical medicine to research laboratories. A result of this incredible transformation is the need for highly annotated tissue specimens, in sufficient quantities to support the growing needs of the cancer research community. Herein we describe various bioinformatics tools used in to support translational research.

Design: These tools can be further classified in to the tools to support the Laboratory Information System (LIS), Tissue Banking Tools, Clinical and research Cancer Registry and Educational Tools.

Results: The various tools that are implemented in our system include the tools for anatomic and clinical pathology LIS such as coPath and synoptic templates for surgical pathology reporting. The data is stored in synoptic templates appear as a summary within the final pathology report, forming a conduit for data transfer to research databases. The tissue banking and pathology tools include Tissue Bank Information system, the caTISSUE Core - a centralized tissue bank, cancer Text Information Extraction System for extracting valuable information from the free text of archival surgical reports, the Clinical Integration Engine to gather information on patient's demography, clinical profile, follow up and pathology diagnosis into a common bioinformatics infrastructure, various organ specific databases such as Co-operative Prostate Cancer Tissue Resource, Pennsylvania Cancer Alliance Bioinformatics Consortium, Colorectal, Head & Neck, Hematolymphoid and Mesothelioma biorepositories with thousands of well annotated tissue samples. The central Cancer Registry Network and Clinical Trial Management System support our research as well as clinical registry network and clinical trials. In addition, it includes various educational tools such as artificial intelligent tutoring system, virtual slide imaging and so on.

Conclusions: These tools eventually forms a common platform for cancer research to expedite progress in clinical and translational research. In addition, these tools provide a concrete infrastructure and resource for education and clinical services within the laboratory information system. Furthermore, applications developed within the tools will provide a novel method to add value to the existing clinical document, archives, and biospecimens.

1625 First Steps in Characterizing the Clinical Phosphoproteome

W Mojica, E Marchetti, J Sun. Univ at Buffalo, Buffalo, NY.

Background: Phosphorylation of proteins is integral to the activity of cellular processes by their regulation of signalling pathways. Aberrant regulation of protein phosphorylation can result in pathologic disease. The first step in identifying potentially significant phosphorylated proteins would be through the examination of normal and neoplastic specimens. Determining if these proteins are clinically significant requires analysis of matched clinical tissue. However, because traditional fixation protocols have been documented to alter the labile phospho-protein bond, alternative approaches are required if the interogation of clinical tissue for phosphoproteins is attempted. Using a recently described non-fixative based cell enrichment method and tandem mass spectrometry, we profiled the phosphoproteome for 3 cases of adenocarcinoma of the colon. This approach can characterize the presence or absence of phosphoproteins in tumors and matched normal clinical tissue.

Design: Non-neoplastic and matched neoplastic colonic epithelial cells were enriched from 3 separate hemicolectomy specimens excised for invasive adenocarcinoma using manual exfoliation with immunomagnetic bead separation. Cells were lysed, proteins resolved by SDSPAGE and then subjected to in-gel tryptic digestion and peptide extraction. Recovered peptides were fractionated using strong cationic exchange chromatography and eluted with wash buffers of increasing salt concentrations. Negatively charged and phosphorylated peptides from each fraction were enriched using gallium chromatography. The eluted phosphopeptides were analyzed by reverse phase liquid chromatography tandem mass spectrometry (Custom Biologics, Toronto, ON). The mass spectra data was analyzed using Sequest and DTASelect software.

Results: Phosphorylated proteins were recovered from each sample. In the normal samples, 355 peptides corresponding to 340 proteins and 278 peptides corresponding to 270 proteins in the tumor fractions were identified. Common to both the normal and neoplastic fractions were 53 phosphoproteins. The remaining phosphorylated proteins were identified either in only the normal fractions (n=287) or neoplastic fractions (n=217). In the neoplastic fractions, 55 of these peptides corresponded to proteins that have yet to be named or characterized.

Conclusions: The lists of phorphorylated proteins identified using this recently described approach provide a basis for the characterization of the phosphoproteome for both non-neoplastic colonic epithelium and adenocarcinoma of the colon.

1626 Implementation of Flow Cytometry Analysis of Myeloid Populations in a High Volume Clinical Laboratory

SA Monaghan, KD Doty, SH Swerdlow, FC Craig. University of Pittsburgh Medical Center, Pittsburgh, PA.

Background: Immunophenotypic abnormalities are well documented in MDS. Yet analysis of maturing myeloid populations is not standardized, some studies used software not commercially available, and patterns of antigen expression vary with stimuli, antibodies, and sample handling. Here, myeloid antigen testing was employed using training strategies and widely available software.

Design: 4-color antibody combinations were run on bone marrow samples: CD14/CD13-CD33/CD45/CD34; CD16/CD13/CD45/CD11b; CD15/CD33/HLA-DR/CD117; CD36/CD64/CD45/CD34. 2 analysis strategies were performed using CellQuest based on population analysis using Boolean logic and simplified back-gating. Antigen intensity, light scatter, and maturation patterns were visually estimated. Antigen intensity was also numerically evaluated (mean fluorescence intensity (MFI) and geometric MFI) for granulocytes (G) and monocytes (M). Orthogonal light scatter for G (OLS-G) was characterized using MFI-ratio of G to lymphocytes. Proportions of maturation stages for G were enumerated. Numeric data was defined as atypical when values were beyond the range and/or 2SD from the mean of controls. Morphology, karyotype and clinical data were also reviewed.

Results: Cases included 4 MDS, 22 with unexplained cytopenias (UC) and 9 controls. Reduced OLS-G was visualized in 3 cases (1 MDS, 2 UC) and supported by numerical assessment. Atypical intensity of at least 1 antigen among G and M was identified in 17 UC and 3 MDS (see table). Variant G patterns for both CD11b vs CD13 and CD13 vs CD16 were present in 7 UC and 1 control, without any MDS showing variation of both. Altered proportions of G maturation subsets correlated with variant G patterns in 4 cases. The control with both G patterns altered was the only case for which processing was delayed by 2 days.

Conclusions: Recognition of visual patterns of antigen expression among maturing myeloid cells comes with experience. Numeric evaluation of well isolated populations helps to substantiate the findings. With increased confidence, many abnormalities can be identified with simple strategies using commercially available software. Delayed specimen processing in 1 control case may have led to altered G maturation patterns, warranting a note of caution.

Increased or decreased antigen intensity

	MDS (n=4)		Unexplained Cytopenias (n=22)	
	Granulocytes	Monocytes	Granulocytes	Monocytes
CD11b	0	1	4	7
CD13	3	0	1	0
CD14	0	0	1	1
CD16	0	0	2	0
CD33	0	0	4	4
HLA-DR	NA	0	NA	3

1627 Clinical Applications of Gene Expression Microarrays: Reproducibility of a Tissue of Origin Test for Metastatic Tumors of Unknown Origin

FA Monzon, CI Dumur, M Lyons-Weiler, CM Sciulli, M Price, L Buturovic, T Rigl, GG Anderson. University of Pittsburgh, Pittsburgh, PA; Virginia Commonwealth University, Richmond, VA; Pathwork Diagnostics, San Jose, CA.

Background: Gene expression profiling is a widely accepted technology in experimental pathology research, but application of gene expression microarrays to address clinically important problems has been slow to come. The Pathwork Tissue of Origin (TOO) test uses the expression of over 500 distinct genes to quantify the molecular similarity between a tissue biopsy sample and fifteen tissues of origin of clinical relevance. Here we describe preliminary results of the clinical validation studies for the Pathwork TOO test performed at two academic molecular diagnostics laboratories and one commercial laboratory.

Design: 33 fresh frozen tissue biopsy samples from poorly differentiated primary and metastatic tumors representing seven (Breast, Bladder, Colon, Lung, Lymphoma, Melanoma and Ovary) of the 15 tissue types were analyzed with the TOO test in three independent laboratories. Assays were performed on Affymetrix GeneChip® arrays per a recommended laboratory protocol. Sample origin (Clinical Truth) was established by a pathologist using standard diagnostic methods. A Tissue of Origin report was generated for each sample. The TOO result was compared against Clinical Truth to establish the performance characteristics of the Pathwork TOO test across the different laboratories.

Results: Standardized gene expression values across the three sites showed linear correlation (r) values from of 0.91 to 0.94 and similarity scores showed correlation of 0.96 to 0.98, showing excellent reproducibility between laboratories. 100% concordance was observed when rescanning arrays on GCS3000 and GCS3000Dx scanners in the same, as well as in different, laboratories.

Conclusions: The Pathwork Tissue of Origin (TOO) test demonstrated robust and reproducible performance across three independent laboratories. This preliminary evaluation demonstrates that there is excellent concordance in the identification of tissue of origin across laboratories. The entire clinical validation study comprises over 500 tissue biopsy samples representing 15 tissue of origin types. We expect to obtain average sensitivity greater than 80% and average specificity greater than 95%. Test accuracy will also be reported.

1628 Feasibility of Top-Down Proteomic Approach Using Paraffin Blocks

M Nassiri, S Ramos, M Nadji, V Vincek, AR Morales. University of Miami Miller School of Medicine, Miami, FL.

Background: Top-down proteomic approach allows separation of cellular proteins based on their subcellular localization. This is crucial for clinically useful biomarker discovery. We have developed a formalin-free molecular-friendly standardized tissue fixation and processing system for clinical tissue specimens. We utilized a Top-Down approach to proteomic studies using tissues processed with this method.

Design: Mouse liver tissue samples were fixed from one to 24 hours in a novel fixative (Molecular Fixative, Sakura Finetek) and processed using a microwave-assisted tissue processor (Xpress, Sakura Finetek). Commercial kits (Bio-Rad and Calbiochem) were used to isolate various subcellular compartments (nuclear, cytoplasmic organelles, cytoplasmic membrane) from the paraffin-embedded tissue. Isolated extracts were further separated on a fluid phase isoelectric focusing chamber (Bio-Rad Micro-Rotofor) and run on SELDI-TOF (Ciphergen) ProteinChips. In addition, samples were subjected to gel electrophoresis. The resulting protein bands were excised, digested and analyzed by Mass Spectrometry to identify specific proteins.

Results: The SELDI-TOF and gel electrophoresis profile was similar between tissues processed by the new molecular friendly system and fresh control sample. Same proteins were identified using mass spectrometry.

Conclusions: A top-down proteomic approach is feasible in paraffin-embedded tissues using the novel molecular fixation and processing. This processing system can be used as a standard platform for proteomic discoveries and clinical studies.

1629 Changes in Antigen Density during Remission Induction in Precursor B-Cell Acute Lymphoblastic Leukemia Detected by Flow Cytometric Immunophenotyping

MS Parab, N Ahmad, SG Fuller, JA DiGiuseppe. Hartford Hospital, Hartford, CT.

Background: The detection of minimal residual disease (MRD) by flow cytometric immunophenotyping (FCM) is an established adverse prognostic factor in patients with precursor B-cell acute lymphoblastic leukemia (pB-ALL). Although changes in antigen expression at relapse compared with diagnosis have been studied extensively, there are comparatively few data regarding changes in antigen density during remission induction, when MRD is commonly assessed.

Design: In a series of 16 cases of pediatric and adult pB-ALL in which MRD was detected by 4-color FCM at one or more times during remission induction, the mean fluorescence intensity (MFI) of several antigens at diagnosis was compared with that seen at day 8, and the last time point during induction at which MRD was detectable. FCM data were acquired using FACSCalibur™ (BD Biosciences, San Jose, CA) flow cytometers, whose stability was verified daily with SPHERO™ Rainbow Fluorescent Particles (Spherotech, Inc., Libertyville, IL), and analyzed using CELLQuest™ and Paint-A-GatePRO™ software (BD Biosciences). The Wilcoxon signed rank test was used to compare the MFI of each antigen at different time points during induction with that seen at diagnosis.

Results: At both day 8, and the last point during induction at which MRD was detectable, significant increases in the MFI of CD20 ($p=0.006$, $p=0.027$) and CD45 ($p=0.043$, $p=0.016$) were seen, while the MFI of CD10 was significantly decreased at these times ($p=0.002$, $p<0.001$). For CD34, a significant decrease in MFI was detectable at the last

point of MRD positivity (p=0.035), but not at day 8. In contrast, expression of both CD19 and CD22 was relatively stable; no significant changes in MFI were observed for either antigen at either time point. Although these changes in antigen density were readily visible in conventional bivariate dot plots, in no case did they preclude the detection of MRD.

Conclusions: In pB-ALL, the density of several antigens commonly studied in the evaluation of MRD by FCM may increase or decrease during remission induction. Recognition that changes in antigen density may occur is important in the analysis of FCM data; however, these changes should not typically preclude the detection of MRD by FCM.

1630 Telepathology as a Continuing Medical Education Tool: Experience at a Multi-Hospital Health System

KP Patel, I Ouansafi, R Robbins, D DeCostanzo, T Bhuiya. Long Island Jewish Medical Center, New Hyde Park, NY; Glen Cove Hospital, Glen Cove, NY; Southside Hospital, Bay Shore, NY.

Background: Currently, the common applications of telepathology include diagnostic, consultative and quality control. The use in continuing medical education is a powerful, yet underutilized application of telepathology. We explored the possibility of using telepathology as a continuing medical education tool in a multi-hospital health system setting.

Design: The study was performed by five participants at different stages of an anatomic pathology career. A senior pathologist (18 years of practice) at an academic medical center (33,000 surgical cases/year) selected classic (but uncommon) and interesting cases from the daily practice. Two pathology residents captured digital images with an Olympus camera. Each week, the residents presented five cases to two pathologists (6-8 years of practice) at community hospitals within the health system with relatively smaller case volume (6000-8300/year). Apollo Telemedicine videoconferencing setup was used for securely sharing the static images and for audiovisual interaction. The senior pathologist provided diagnostic clues, practical guidelines and status of current literature on each entity. A total of 50 instructive cases representing multiple specialties were shown over a period of 10 weeks.

Results: Both the participating pathologists found the number of images (Range: 5 to 12) optimal for all cases. Both the participants saw 41 (82%) entities for the first time in the last 3 years. A total of 24 (48%) entities were seen for the first time ever by both the participants, although they were aware of 15 of them. The participants became aware of 13 new entities. Both expressed confidence in diagnosing 38 (76%) entities with reasonable certainty in the future. Only 1 case was identified as difficult to diagnose in future by both. Both expressed a need for consultation with another pathologist while making diagnosis on 12 (24%) cases. Multiple other benefits were obtained such as the generation of an image bank, the addition of all the cases to the teaching slides, and renewed awareness among the staff about the utility of telepathology system.

Conclusions: Telepathology can be a very useful continuing medical education tool, both for residents and practicing pathologists, especially in the multi-hospital health system settings. This adds a new dimension to the current utility of telepathology as a diagnostic and quality control tool.

1631 Semiautomated Method for Generating Widefield Digital Image Mosaics from Bright-Field and Fluorescence Microscopy

VB Reddy. University of Alabama at Birmingham, Birmingham, AL.

Background: Widefield images of the pathological sections and smears are extremely useful in morphometry, morphology studies, delineating immuno architecture and intracellular staining patterns. We created widefield microscopic images (mosaics) by Photo-merging software from series of digital microscopic images individually acquired under visual control. Image mosaics are larger than field of view of the microscope or camera, and are generated by blending user defined microscopic fields without the loss of resolution. This method allows complete flexibility of image acquisition at all magnifications (low and high), and automated "image-stitching" to produce digital widefield images utilizing the existing microscopes with manual stage controls and digital camera systems.

Design: All images are acquired through Nikon DS-5M-DS-L1 control unit (Nikon, Inc, Melville, NY) digital camera mounted on a research grade microscope with plan apochromatic objective lenses (4x, 10x, 20x, 50x oil, 100x oil). Eyepiece grid (9 square grid) reticle was used to select series of overlapping (10-20%) images of user defined fields (4x, 20x, 50x oil for bright-field and 50x/100x oil for fluorescence). Peak-hold photometry with exposure lock was used during image acquisition. Images are processed by Photomerg® plug-in, Adobe Photoshop CS2 (Adobe, Inc, San Jose, CA) using advanced blending option. Final processed images are saved in TIFF / JPEG formats.

Results: Image mosaics of follicular lymphoma (n 11) and mast cells infiltrates (n 5) of the bone marrow are obtained; these are on average 400% larger than single microscope objective field of view. Mosaics are of high resolution without distortion or loss of cellular details and possible to do multiple studies. Details of Hematoxylin & eosin morphology, immuno-architecture (Dako mouse anti human antibodies, CD20, CD10, Bcl-2) and positive FISH (Vysis) t(14;18) areas in the lymph node are easily documented. Similar immuno architecture of mast cell infiltrates in the marrow by CD117 staining pattern was established. Morphometry of the full length of bone marrow biopsies including bone cortex measurements are made.

Conclusions: Photo-merging software allows seamless blending of user defined digital images to produce high quality widefield microscopy image mosaics at any magnification. Morphometry and immunoarchitecture evaluations are possible on these images. Additionally, this is a low cost approach using current existing microscopes and digital cameras.

1632 Conversion of Tissue Chromogenic Staining to "Virtual Flow Cytometry" by iHCFLOW System

D Rezania, HD Cualing, E Zhong, L Li. HL Moffitt Cancer Center Research Institute, USF, Tampa, FL; IHCFLOW-GreenGreat; Dianzi University, Hangzhou, China.

Background: We present a novel method that converts tissue immunohistochemistry to flow cytometry-like result. The objective was to recreate the functionality of a flow cytometer but instead of using the requisite cell suspension uses immunostained microscopic tissue slides. It is a fully automated, fast, accurate method that analyzes a 512 x 474 RGB image 2-3 s from analysis to a dot-plot display. We present features that allow segmentation of membrane and nuclear stained lymphocytes useful in daily hematopathology and pathology practice.

Design: We provide correlation coefficient and CV data to show high accuracy of the prototype software using several antibodies, varied image frames, varied rheostat settings, and with varied microscope systems and operators.Previous validation is in Clinical Cytometry B, Oct. 2006. DATA: a total 128 image frames with 218,192 digital cell objects using CD3,CD4,CD5,CD8,CD10,CD23,CD138, Bcl-1,Kappa, Ki67, Lambda, Mum1, P53. Using 20x, we varied lighting intensities from 4.0 to 7.0 rheostat(= 10-192 intensity units) and using a small 512 X 474 or large image frames, from two kinds of microscopes, we additionally compared acuracy results.

Results: Concordance: Correlation Coefficients between 1) small vs large frames: r . 9760 to .9484; 2) different microscopes and CCD setup: r 0.9694; 3) CV of percent positive: 0.028 to 0.069 using bright to dark lighting. With accuracy of results in relation to parameter epsilon, we obtained a strong positive correlation between the epsilon parameter that correlates with % + and our iHCFLOW results that ranges from r 0.7738 to 0.5091 using 14 antibodies and a lower correlation coefficient using pixel based thresholding: isodata autothresholding r 0.1267 and isodata with manually adjusted thresholding r 0.4235.

Conclusions: We observed high accuracy and invariance to varied conditions of acquisition. We obtained robust results of both positive and unstained lymphocytes of the same class with a "virtual flow cytometry" dot plot reporting, 2)invariance using many antibodies, 3) high concordance of small and large image frames 4) high concordance between two different microscopes and CCD setup and 5) invariance to changes in rheostat light intensity. These results suggest applicability in daily microscopy workflow of pathologists and scientists with wide latitude, fast performance, accurate high throughput reporting *ala* flow cytometry.

1633 Automated Determination of Bone Marrow Cellularity

E Sagatys, H Cualing, L Kang, E Zhong, L Moscinski. H. Lee Moffitt Cancer Center at the University of South Florida, Tampa, FL; IHCFlowGreenGreat.

Background: Determining bone marrow cellularity is often a subjective estimation with great interobserver variation. A rapid, accurate, reproducible method would be desirable for pathologists who regularly examine bone marrow biopsies.

Design: Using public domain image analysis software ImageJ (NIH W Rasband, v1.34m) and advanced user-defined algorithms provided by iHCFlowGreenGreat, we examined 37 bone marrow core biopsies stained with hematoxylin and eosin and periodic acid shift stains obtained by 4 pathologists using 4 different microscopes color CCD setup. Normal marrows and those involved by both benign and malignant processes including anemia, status post chemotherapy, myelodysplastic and myeloproliferative disorders, leukemias, and lymphomas are examined. The raw images and the corresponding segmented marrow cellularity are stored for evaluation. The images were either PAS or H and E stained and either 20x or 40x. All bone trabeculae are excluded by each operator. Analysis takes 2-3 seconds using a Pentium 1.6 Gigahertz CPU, with a conventional color CCD camera and the Twain facility software.

Results: Nine out of ten cases examined demonstrated 100% accuracy in determinating cellularity using the image analysis software. The correlation coefficient of pathologist and Bone Marrow Cytometer using linear regression(Instat Graphpad) is r=0.84, $p<0.0001$ with four outliers in 37 cases. Initial problematic images, hypo and hypercellular marrows, are resolved with nuclear segmentation in the hypocellular marrows and accurate nuclear and cytoplasmic segmentation in the hypercellular marrows. The hypocellular marrow at day 14 post chemotherapy was segmented excluding the serous stroma and extracted nucleated cells only. In some PAS stained hypercellular marrows, the image analysis is currently problematic with images of 40x but not in the 20x objective fields.

Conclusions: We found the automated image analysis technique to be useful, rapid and accurate way to extract bone marrow cellularity and provide a cell to fat ratio. We believe an accurate, objective, rapid measurement of bone marrow cellularity would be beneficial to practicing pathologists.

1634 Detection of JAK2 Mutation Status by Post-PCR Fluorescent Ligase Detection Reaction and Flow Cytometric Bead-Based Analysis

M Salama, M Mariappan, I Chen, A Chakerian, S Merchant, D Viswanatha. Univ. of New Mexico, Albuquerque, NM; Veterans Administration Hospital, Albuquerque, NM; Stanford Univ, Stanford, CA.

Background: The 1849G>T (V617F) *JAK2* gene activating point mutation was recently identified in a substantial subset of classical chronic myeloproliferative disorders (CMPD) excluding chronic myeloid leukemia. We describe a novel post-PCR fluorescent DNA ligation detection reaction assay (f-LDR) for sensitive and specific detection of the *JAK2* V617F mutation.

Design: Positive control DNA was obtained from the HEL92.1.7 cell line (ATCC, Manassas, VA) that carries a homozygous V617F *JAK2* mutation. Negative (wild type) control DNA was obtained from random blood donor leukocytes. Samples from 12 CMPD patients with previously identified *JAK2* mutations (by clinically-validated LightCycler assay) were studied, in addition to 6 cryopreserved cases of B-lineage acute lymphoblastic leukemia (ALL) and 6 paraffin-embedded tissue biopsies of Hodgkin lymphoma. Analytic sensitivity was determined using serial 2-fold dilutions of HEL

DNA in normal leukocyte DNA. The *JAK2* 1849G>T mutation site region was amplified by PCR. Following PCR, an aliquot of product was subjected to multiplex f-LDR using upstream discriminating 5'labeled 6-FAM mutant-specific (mut) and CY5 wild type (wt) primers and a common adjacent 3' biotinylated downstream primer (com). Following f-LDR, products were incubated with streptavidin-coated microbeads and subjected to 2-color flow cytometry to detect mutant and wild type fluorescent sequences.
Results: HEL cell line dilution studies revealed 3% sensitivity for detection of mutated *JAK2* alleles. No cross-hybridization (e.g. mut primer with wt sequence or vice versa) was observed using normal leukocyte and pure HEL DNA in the f-LDR assay. All 12 negative control DNA samples were positive with the wt primer set and negative with the mutant primer set. All 12 known *JAK2*+ CMPD cases were mut primer set positive by f-LDR (100% diagnostic specificity). 10/12 CMPD cases also showed variable wt signal indicative of mixed *JAK2* zygosity. Two CMPD samples showed strong positive mut signal but absent wt signal (like HEL DNA), consistent with homozygous *JAK2* mutation.
Conclusions: The f-LDR assay was 100% specific for detection of *JAK2* mutations in CMPD and demonstrated acceptable analytic sensitivity for clinical use. No *JAK2* mutations were detected in the subset of HL cases analyzed, suggesting that mutation per se is not involved in *JAK2* de-regulation in this neoplasm.

1635 Comparison of Three Different Chromatic Dyes for the Measurement of Phosphorylated Ser727-Stat3 by Slide-Based Cytometry

J Schwock, A Keys, JC Ho, DW Hedley, WR Geddie. University of Toronto, Toronto, ON, Canada; Cambridge, MA.
Background: The measurement of phosphorylated signaling proteins may be increasingly used for the pharmacodynamic monitoring of novel molecular targeted therapeutics. We have previously shown that differences in signaling pathway activities can be detected in fine-needle aspiration specimens. Differences in chromatic staining due to changes in (phospho-)epitope abundance can be measured based on laser light loss and quantified by slide-based cytometry. However, the applicability of different chromatic dyes for this approach has not yet been addressed.
Design: We used a xenograft specimen series of fine-needle samples subjected to delayed formalin fixation and the corresponding excised tumors to evaluate three different chromatic dyes (DAB, AEC, NovaRed) in immunohistochemistry for Ser727-Stat3 with hematoxylin counterstaining. Each dye was evaluated for its capability to produce differential signal intensities on an iCyte™ Research Imaging Cytometer. The results were compared to a biological trend previously determined by visual inspection and direct immunofluorescence. We tested if compensation for spectral overlap from the nuclear counterstain could be performed sufficiently for each dye. A multiplexed analysis of slides stained with >2 chromogens was tested for the combination VectorRed or NiDAB/DAB/ hematoxylin.
Results: All three chromatic dyes produce similar signal intensities as measured by corrected blue laser light loss. The observed staining intensity ratios compared favorably with the known biological trend. Additionally, we were able to obtain efficient compensation for spectral overlap with each of the three dyes. Nova Red produces a stronger relative intensity ratio when used with random sampling of the tissue. However, this trend was not seen with cell-based (nuclear) sampling. An increased amount of green tissue auto-fluorescence was seen with AEC substrate which may be due either to sample processing or the substrate itself.
Conclusions: DAB, AEC, and Nova Red work equally well for slide-based cytometry based on laser light loss measurement. Nova Red provides a slight advantage in signal intensity ratio when using the random, but not the cell-based sampling method. The measurement of signaling pathway activities in small biopsies of solid tumors may replace the semiquantitative scoring performed by a pathologist and provide an early pharmacodynamic read-out for the efficacy of a targeted treatment approach.

1636 A New Technique for Assessment of Tumor Cell Viability for Chemo-Response Testing: A Concordance Study

J Silverman, J Heinzman, S Brower, J Bush. Allegheny General Hospital, Pittsburgh, PA; Precision Therapeutics, Inc, Pittsburgh, PA.
Background: Chemo-response (CR) testing is now being performed at commercial laboratories to better assist oncologists in selecting appropriate chemotherapeutic regimen for treating cancer patients. A viable malignant epithelial cell population is required for *ex vivo* CR prediction. Currently, immunofluorescence (IF) studies for epithelial antigens are performed to determine if a malignant epithelial cells rather than fibroblastic overgrowth are present. We evaluated whether the cytopathologist's examination applying conventional cytomorphologic criteria and immunohistochemical (IHC) studies for epithelial differentiation can be useful in determining malignant cell viability for CR studies.
Design: Fifty-one human tumor specimens (14 breast, 8 colon, 14 lung, 10 ovary and 5 other) were established and maintained in short-term primary culture. Cytospins of the cell suspensions were prepared at the conclusion of the culture period and stained with Diff-Quik and Papanicolaou stain and IHC studies were performed for AE1/3, Cam 5.2, CK7, EMA and CK20 and compared with standard IF studies performed at a commercial laboratory. Positive IF for epithelial antigens (AE1/3 and Cam 5.2) was utilized to confirm that greater than 65% of the culture cells represented a viable epithelial cell population for CR studies. These results were compared with the cytomorphologic and IHC staining.
Results: There was concordance between IF and cytologic/IHC in 42/51 cultures. Cytologic/IHC studies identified two positive cultures which failed IF testing. There were two cytomorphologic/IHC failures which passed IF examination. Five cultures showed lack of malignant cells in both the cytologic/IHC and IF studies. Concordance between IF and cytology/IHC had a kappa of 0.669 with a good strength of agreement.
Conclusions: Pathologists are increasingly involved in providing chemotherapeutic response predictions of malignancies in routine clinical practice. CR testing is now also being utilized to help select the most appropriate chemotherapeutic agents to treat a variety of malignancies. We believe that the cytopathologist can have an role in assessing the presence of malignant cells in cultures used for CR testing by applying standard diagnostic cytomorphologic criteria of malignancy and IHC studies. The cytologic/IHC studies also offers advantages over IF studies which is limited by subjectivity due to interobserver variability and variable staining intensity of the cultured cells.

1637 Intra-Observer Reliability of Whole Slide Images in Pathology Quality Assurance Studies

N Suh, D Jukic, J Ho, JR Gilbertson, J Fine, L Anthony, R Silowash, AV Parwani. University of Pittsburgh, Pittsburgh, PA; Washington University, St Louis, MS; Case Western Reserve University, Cleveland, OH.
Background: Whole Slide Imaging (WSI) is an evolving technology which has the potential to change the way surgical pathology is practiced today. Quality Assurance(QA) is an important part of validation of these automated system before implementing them in daily pathology practices. In our previous study, we reported a good consensus between WSI diagnosis and microscope based glass slide diagnosis compared with the original pathology report. However, it is also important to evaluate intra-observer variation of the diagnosis (self agreement across the condition; glass slide v.s. virtual image) for the quality assurance of the WSI system.
Design: Twenty four entire cases (including 47 surgical parts and 391 slides) from the genitourinary surgical bench were selected randomly and were scanned by Aperio T2(Aperio Technologies, Vista, Calif) whole slide image scanner. Four anatomic pathologists participated in this study. Each pathologist signed out assigned cases by glass slides while other pathologists signed out the corresponding whole slide images. During the sign out, the pathologists were required to fill in the QA form and evaluate diagnostic concordance, confidence, case complexity, and time to complete the case. After that time, approximately 20% of the cases from this study were assigned to the same pathologists for intra-observer reliability assessment.
Results: 15 cases with 234 images were evaluated across the condition. The diagnostic confidence for both the glass and WSI interpretation was high. Of the 15 cases, 12 were reported as high confidence, whereas 3 were reported as medium confidence. There were no disagreements by the pathologists. The diagnosis remained unchanged after reviewing the corresponding WSI or glass slides in all 15 cases which were also concordant with the primary diagnosis in original pathology report.
Conclusions: The diagnostic confidence as well as intra-observerr reliability for the WSI was high in the cases selected for assessment. Although the study was done on a small number of cases, the results are encouraging and support Whole Slide Imaging as a useful tool in pathology practices especially for QA studies in surgical pathology. This new and rapidly evolving technology has the potential to be useful in multiple facets of an anatomical pathology practice.

1638 The Evaluation of P504S, HMW CK and p63 Using a Triple-Antibody Cocktail with a Triple Chromogen Staining Procedure

D Tacha, M Teixeira. Biocare Medical LLC, Concord, CA.
Background: The use of P504S as a positive marker and HMW CK and p63 as negative markers in prostate cancer has been shown to improve diagnostic performance. In cases of limited tissue, the problems of studying small lesions in prostate needle biopsies with multiple immunohistochemical stains may prove useful. We therefore assessed the usefulness of a triple-antibody cocktail using P504S, a high molecular weight cytokeratin (HMW CK), and p63. A triple stain protocol was employed using three different chromogens. In prostate carcinoma, red cytoplasmic granular staining (P504S) was detected in the malignant glands and cells. In adjacent nonmalignant glands, a dark brown cytoplasmic (HMW CK) staining was present in the basal epithelium and a purple stain was present in basal nuclei (p63). All malignant glands were negative for basal cell staining. All benign glands adjacent to malignant glands were recognized easily by basal cell markers with little or no P504S expression.
Design: Prostate biopsies were formalin-fixed and embedded in paraffin. A cocktail of rabbit polyclonal P504S and a mouse anti-HMWCK was applied for 30 minutes followed by a cocktail detection for 30 minutes. DAB and Fast Red were applied sequentially. A denaturing solution was applied for 5 minutes and then mouse anti-p63 was applied for 30 minutes. A conjugated goat anti-mouse-HRP was applied for 30 minutes and purple chromogen was used to provide the third color. The assay was performed manually and on an automated stainer.
Results: P504S (red) was detected in the malignant glands and cells. In adjacent nonmalignant glands, HMW CK (brown) staining was present in the basal epithelium and p63 in basal nuclei (purple) . All malignant glands were negative for basal cell staining. All benign glands adjacent to malignant glands were recognized easily by basal cell markers with little or no P504S expression. No benign glands were simultaneously positive for P504S and negative for basal cell markers. There were no differences in intensity and numbers of positive glands when comparing the triple-stain procedure with a single stain protocol for each specific antigen of interest.
Conclusions: Our results indicate that immunohistochemistry with a 3-antibody cocktail and triple chromogen is a simple and easy assay that can be used as a routine test. This overcomes the problems of studying small lesions in prostate needle biopsies when multiple immunohistochemical stains are required, and in cases of limited tissue.

1639 A Rapid Five-Step Mouse on Mouse Double Stain Procedure

M Tacha, D Lobo, J Vargas. Biocare Medical LLC, Concord, CA.
Background: If a mouse monoclonal antibody is desired for immunohistochemical detection on mouse tissues, a mouse on mouse detection system is usually employed. If a double stain is desired, then a sequential staining protocol using a denaturing step can be used. However, certain tissues may require an avidin-biotin blocking step. To circumvent these problems, a new sequential 5-step mouse on mouse double stain protocol has been developed that incorporates avidin-biotin blocking steps into a

blocking reagent and antibody diluent. A biotinylated primary antibody complex is cocktailed with an unlabelled rabbit antibody and incubated. This was followed by a sequential cocktail of streptavidin-HRP and a biotin-free goat anti-rabbit alkaline phosphatase. Chromogens were applied sequentially for two-color staining. Double staining was easily achieved in five sequential steps, thus eliminating avidin-biotin blocking and a denaturing step.

Design: Tissues were formalin-fixed and embedded in paraffin. The protocol incorporates avidin-biotin blocking reagents in the blocking step and in the antibody diluent, respectively. A biotinylated mouse primary (Fab fragment antibody complex) is cocktailed with an unlabelled rabbit antibody. The antibody complex was then incubated for 30-60 minutes, followed by a sequential cocktail of streptavidin-HRP and a biotin-free goat anti-rabbit alkaline phosphatase. DAB and fast red chromogens were applied sequentially. Several cocktails were tested including PCNA and CD3, PCNA and smooth muscle actin and neurofilament and GFAP. Tissue were stained manually and on an automated stainer.

Results: Two-color staining was easily achieved in five sequential steps, thus eliminating avidin-biotin blocking and a denaturing step. All antibody combinations stained the correct target antigen and all negative controls were negative. The double stain procedure took approximately 2 to 2.5 hours to completion. PCNA and Smooth Muscle Actin (Fig # 1).

Conclusions: Although a limited number of antibody combinations were tested, this mouse on mouse double stain procedure shows promise for many potential antibody cocktails.

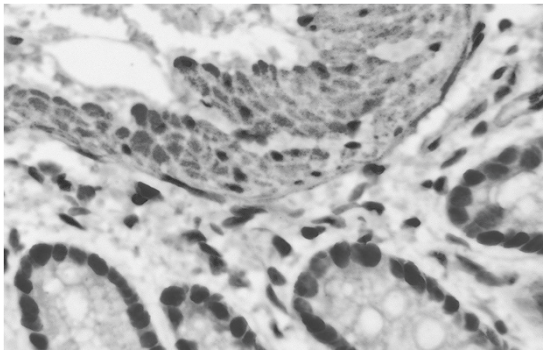

1640 Structured Data Entry and Reporting Using Misys Healthcare CoPathPlus: A Two Year Experience

JM Tuthill, P Tranchida, A Ormsby, RJ Zarbo. Henry Ford Health System, Detroit, MI.

Background: Structuring the data entered on anatomic pathology reports has long been a goal for clear reporting of pathology diagnoses as well as other case features. This has typically been accomplished by use of text templates, inserted in the various sections of a report and populated with case specific information. This results in communicating clear and consistent text for similar diagnostic entities. However, such templates are still effectively "free text" and do not result in database specific field population for the elements in question nor are they able to exploit advantages of database technology for queries. Working with Misys Healthcare we helped develop and implement structured data entry and reporting modules that lead to database driven structuring of diagnostic pathology information.

Design: Tables were added to the CoPathPlus database allowing the population of a structured data checklist consisting of structured categories each of which is comprised of specified data elements. The default structured data dictionary elements provided by Misys were replaced with Henry Ford Hospital synoptic reports that have been in use for over a decade. A particular checklist is added to a CoPathPlus case and associated with its part(s). Once added to a case, the associated checklist categories are populated with specific elements through pick lists allowing for structuring of the case data. A comment field is also provided.

Results: Since implementation of the system we have structured over 3000 cases. Once the required information is available, adding the checklist and populating the required data can be accomplished in less than one minute. The checklist must be fully populated for each category prior to signing out the case, which reduces potential for omission error. Once entered, structured information can be mined using reports built against the database and can be tailored to categories of interest. Reports run rapidly and are highly specific, compared to natural language or SNOMED queries. The synoptic report can be formatted to appear in a concise summary list in the case report.

Conclusions: Structuring pathology data and creating a simple pick-list driven interface has resulted in a highly efficient way to enter diagnostic information. Data retrieval from the system is highly specified and brisk. Transcription and omission errors have been reduced with significant time savings and process improvement. This tool can also be used for non-neoplastic cases, and we are currently developing these checklists.

1641 Combining Different Techniques To Construct Paraffin Tissue Microarrays of Superior Quality

UF Vogel, BD Bueltmann. University Clinic, Eberhard-Karls-University, Tuebingen, Baden-Wuerttemberg, Germany.

Background: Several different techniques are nowadays available to construct paraffin tissue microarrays (PTMAs). The mostly used Beecher technique works with paraffin tissue core biopsies (PTCBs) as small as 0.6 mm in diameter. However, a solid contact between the paraffin of the PTMA and the PTCBs is not achieved. The techniques published by Mengel et al., Wilkens and Ni Chen only apply PTCBs as small as 1.5 mm or 1.0 mm, respectively, but comprise a melting process resulting in a solid contact between the PTMA and the PTCBs. As proved by Mengel et al., this solid contact can dramatically reduce the loss of PTCBs at sectioning and staining. In order to benefit from the melting process when working with PTCBs 0.6 mm in diameter, we combined the Beecher technique with the technique of Wilkens and Ni Chen.

Design: PTMAs with PTCBs 0.6 mm in diameter were constructed according to the Beecher technique by applying PTCBs to preformed holes in a PTMA. After completion, the PTMAs were precut with an ordinary microtome in order to get a smooth surface of the PTMAs. Then, as patented by Wilkens and published by Ni Chen, a double-sided adhesive tape attached to x-ray film was mounted on the surface of the PTMAs. Then these tape-film-PTMA sandwiches were put into ordinary metal molds and melted. After resolidification the sandwiches were removed from the molds and the tape-film platforms were peeled off the PTMAs.

Results: At sectioning and staining the loss of PTCBs was reduced by the solid contact of the paraffins of the PTMAs and the PTCBs as already published by Mengel et al., but could not be reduced to zero.

Conclusions: Combining different techniques to construct PTMAs can improve the quality of PTMAs, especially by melting high density PTMAs using PTCBs 0.6 mm in diameter.

1642 Identification of Amyloid Proteins in Formalin Fixed Paraffin Embedded Biopsy Specimens by a Novel Method Based on Mass Spectrometry Following Laser Dissection and Capture

JA Vrana, JD Gamez, TB Plummer, HR Bergen, A Dogan. Mayo Clinic, Rochester, MN.

Background: The management of systemic amyloidosis relies on the treatment of the underlying etiology and differs radically for different amyloid types. Therefore, given that at least 25 different proteins have been associated with amyloidosis, accurate identification of proteins deposited as amyloid fibrils is an important clinical problem. In this study, we describe a novel method that can characterize amyloid subtypes using mass spectrometry (MS) on formalin-fixed paraffin embedded (FFPE) tissues.

Design: The study used FFPE tissues from four cases of amyloidosis, previously characterized as transthyretin (TTY), serum amyloid-associated protein (SAA), and immunoglobulin light chain lambda (IGL) and kappa (IGK). Laser dissection and capture of amyloid plaques from sections of FFPE that were previously stained with Congo Red or Hematoxylin was performed. Proteins were extracted, digested with trypsin and identified following MS/MS analysis.

Results: Mass spectrometry correctly identified each of the 4 types of amyloidosis analyzed with 100% specificity and sensitivity. In addition, peptide sequences containing mutations in the TTY were identified that may allow further classification into senile or familial amyloidosis. Amino acid rearrangements in IGL and IGK were also seen. Additionally, Serum Amyloid P component (SAP) was also identified as a constituent of the amyloid deposition.

Conclusions: The use of laser dissection and capture from paraffin embedded biopsies and subsequent analysis by mass spectrometry allows identification of the type of amyloid protein deposited with high specificity and sensitivity. This method promises to be a clinical test for accurate identification of amyloid proteins in routinely processed biopsy specimens and overcomes many of the specificity and sensitivity issues associated with current methods such as immunohistochemistry.

1643 Evaluation of *In Situ* Hybridization as a Means of Assessing Immunoglobulin Light Chain Restriction in Plasma Cell and B Cell Neoplasia

BA Webber, C Cohen. Veterans Administration Medical Center, Atlanta, GA; Emory University, Atlanta, GA.

Background: Diagnosis of B cell neoplasia often requires demonstration of immunoglobulin light chain restriction as an indication of clonality. Establishing light chain restriction by flow cytometry is occasionally precluded when fresh tissue is unavailable or if neoplastic infiltrates are patchy. Immunohistochemical light chain studies are often hindered by high background staining. In situ hybridization (ISH), using probes for kappa and lambda mRNA, has emerged as an alternative to immunohistochemistry. We assessed kappa/lambda ISH performance on B5-fixed, decalcified marrow cores and formalin-fixed tissues in a variety of B cell/plasma cell neoplasias, and benign hyperplastic conditions.

Design: Sections of archived paraffin embedded tissues were stained via automated in situ hybridization using pre-diluted kappa and lambda probe on a Bond-max Autostainer (Vision BioSystems). Cases included 18 plasma cell dyscrasia/myeloma marrows, 2 soft tissue plasmacytomas, 3 diffuse large B cell lymphomas, 2 follicular lymphomas, 6 marginal zone lymphomas, 1 polyclonal marrow plasmacytosis, 1 Castleman disease, and 12 tonsillar follicular lymphoid hyperplasia. All marrows were B5-fixed and decalcified, while the remaining cases were formalin-fixed. Two pathologists reviewed ISH slides, and correlated findings with previously documented light chain restriction in the neoplastic cases.

Results: ISH revealed light chain restriction in agreement with recorded flow cytometry results in only 3/18 (17%) of the marrow plasma cell neoplasia cases. Of the formalin-fixed, non-decalcified neoplastic specimens, appropriate light chain restriction was only apparent in the 2 plasmacytoma cases. ISH results, thus, were indeterminate in 26/31 (84%) of all neoplastic cases. In the 11 lymphoma cases, staining was only seen in background polyclonal plasma cells and not in the neoplastic population or in mature lymphocytes. The benign tonsils and the Castleman disease case showed polyclonal staining in plasma cells only. Nonspecific nuclear staining with both kappa and lambda probes was noted in B5-fixed, decalcified, but not formalin-fixed, specimens.

Conclusions: Kappa/lambda ISH appears ideally suited to assess clonality of plasma cell infiltrates in formalin-fixed tissue. However, this methodology is only rarely effective in B5-fixed, decalcified marrow specimens and does not appear useful in evaluating

mature B-cell lymphomas.

1644 Flow Cytometry Immunophenotypic Analysis of Anaplastic Large Cell Lymphoma

EX Wei, JL Jorgensen, LJ Medeiros, P Lin. UT MD Anderson Cancer Center, Houston, TX.

Background: Anaplastic large cell lymphoma (ALCL) of T or null cell type is usually diagnosed by routine histology and demonstration of CD30 expression by immunostaining. The expression patterns of various T-cell related markers in ALCL have not been well studied. Flow cytometry immunophenotyping (FCI) is increasingly employed to evaluate samples such as fine needle aspiration (FNA) when routine histology is not always available.

Design: We searched for cases of ALCL from the files of the pathology service that were analyzed by FCI from 2001 to 2006. The diagnosis of each case was confirmed by excisional biopsy and appropriate immunostains including CD30 and ALK. The panel of FCI included CD30-PE, CD3, CD14 and CD45 in all cases, and various combinations of CD2, CD4, CD5, CD7, CD8, CD16, CD25, and CD56 in subsets of cases.

Results: We identified 17 cases, 9 biopsy specimens, 7 FNAs and 1 pleural fluid. On forward/side scatter plot, the neoplastic cells were large, falling in the region of monocytes. Each case was positive for CD45 (bright) and CD30; and negative for CD14, CD16, and CD56. The frequency of other T-cell associated markers expressed in decreasing order was: CD2, 7/7 (100%); CD5, 8/13 (62%); CD4, 8/14 (57%); CD3, 9/17 (53%) (one case being cytoplasmic only); CD7, 4/8 (50%); CD25, 2/4 (50%); and CD8, 2/14 (14%). 14 cases expressed at least one T-cell associated marker. 2 cases revealed no expression of any T-cell associated markers despite demonstrable CD3 expression by inmmunostaining. 1 case was negative for all T-cell markers assessed by FCI and was considered of null cell type. ALK was positive by immunostain in 7 of 13 cases (54%). The expression patterns of markers assessed were not significantly different between ALK+ versus ALK- tumors.

Conclusions: The neoplastic cells in ALCL have a scatter pattern similar to that of monocytes, and are brightly positive for CD45 but negative for CD14. The most frequently expressed T-cell associated markers in ALCL are CD2 followed by CD5 and CD4. There is no significant difference in the flow cytometry immunophenotypes of ALK+ and ALK- tumors.

1645 Virtual Microscopy in Medical School Education: Four Years of Experience at Loyola Chicago's Stritch School of Medicine

EM Wojcik, P Pioro, T Kristopaitis, M Sheehan, JM Lee. Loyola University Medical Center, Maywood, IL; Stritch School of Medicine, Maywood, IL.

Background: Virtual Microscopy (VM) is the technique of digitizing a glass microscope slide that can be viewed on any personal computer, which acts as a microscope. VM allows simultaneous viewing of a standardized slide by many users either in the classroom or at home. The aim of this study is to summarize four year experience with this novel technology at the Stritch School of Medicine and present students' perspective.

Design: VM was made available for medical students in 2001 and originally was used along with traditional microscopic slides and microscopes. From 2002 only VM was used in laboratory sessions. At the end of each semester, students were asked how VM reinforced their learning of the material presented in the lab sessions.

Results: The results are based on 931 responses (range of responders/semester: 85-140) obtained at the end of eight semesters. The overall evaluation of VM was very positive (average score 3.8 in a scale of 1-5). There was no significant difference in grades between eight different semesters. In a scale 1-5 (1; strongly disagree – 5; strongly agree), the highest number of students scored VM as 4 (35%) and 5 (28%). Score 3 was assigned by 21% of students, score 2 by 8% and score 1 also by 8%.

Conclusions: Virtual Microscopy has been embraced by the medical students from the time of it implementation. VM proved to be a useful educational tool to be used in microscopic laboratory sessions. It allows standardization and the viewing of slides at any location. This technology has enhanced pathology education.

1646 Interactive Case-Based Exercises in Pathology Education

JT Woosley, H Reisner. University of North Carolina School of Medicine, Chapel Hill, NC.

Background: Background. Conventional approaches to teaching pathology to medical students and residents have limitations. Lectures, texts and atlases are limited in their ability to actively engage the student and permit interactive learning. *Flash* is a widely used graphics/animation system (Adobe) designed to produce multimedia content convenient for dissemination to multiple computer platforms and other portable media-capable devices. Media can be created that allows the student to interact with content and receive feedback in a way impossible to obtain with traditional printed texts. Sophisticated productions using *Flash* can require expert design and programming capabilities which may not be readily available. *Camtasia Studio* (Techsmith) allows for facile production of interactive multimedia pathology tutorials incorporating *Flash* technology without requiring *Flash* expertise.

Design: Design. *Camtasia Studio* has been used to create interactive multimedia *Flash* case-based tutorials for pathology education. *Camtasia Studio* provides a "plug-in" for *PowerPoint* allowing rapid storyboarding that incorporates audio, annotations and animated sequential magnification of image areas containing diagnostic features. Such sequential magnification allows emphasis of areas of interest without producing excessive screen clutter. *Flash* based multiple-choice questions follow the multimedia presentation, testing comprehension and adding additional pathologic detail. Presentations can be linked to virtual slides (the image source used) for additional study.

Results: Results. Over 100 video pathologic tutorials have been created, covering a variety of pathologic processes. The tutorials have been used in our 2nd year GI organ system based block and have received excellent feedback from students, including receipt of the Best Second Year Course Award.

Conclusions: Conclusions. Multimedia pathology tutorials paired with virtual slides are extremely effective because they closely mimic "traditional" instruction at the microscope. They also offer the significant advantage of allowing remote teaching at any time or place convenient for the learner. Tutorials can be compressed into a variety of multimedia formats and can be streamed for web delivery, provided on CD for distribution or used on media-capable portable devices.

1647 Mitotic Rate by PHH3 Immunostain Is a Stronger Predictor of Metastasis in Malignant Melanoma Than Mitotic Rate by Routine H&E Stain

KE Youens, KB Johnson, JW Turner, KR Perkinson, RT Vollmer, MA Selim. Duke University Medical Center, Durham, NC; Durham VA, Durham, NC.

Background: Tumor mitotic rate has been established as a predictor of metastasis in malignant melanoma. Mitotic rate is now determined by counting mitotic figures on hematoxylin- and eosin-stained (H&E) sections, a process that can be time-consuming and difficult in some cases. The monoclonal antibody anti-phosphohistone-H3 Ser28 (PHH3) binds to histone H3 in the highly phosphorolated state acquired in cells undergoing mitosis, allowing their specific identification. This study was done to explore the utility of a PHH3 immunoperoxidase stain for determination of mitotic rate in melanoma, and to determine whether mitotic rate by PHH3 is superior to mitotic rate by routine H&E for predicting metastasis in malignant melanoma.

Design: Immunohistochemical staining for PHH3 was performed on paraffin-embedded tissue from 34 cases of malignant melanoma (17 from patients with metastases and 17 from patients without metastases). For each case, the mitotic rate was determined on a PHH3-stained slide and an archival H&E slide from the same tissue section. Four observers determined mitotic rate by counting mitotic figures, as defined by standardized criteria. Statistical analysis primarily consisted of logistic regression analysis to test the association between metastasizing malignant melanomas and staining for mitotic rate by H&E and mitotic rate by PHH3.

Results: In most cases, PHH3 allowed for easy identification of areas of brisk mitotic activity and helped distinguish between true mitoses and apoptotic or necrotic cells. Using H&E, the average mitotic rate for all cases was 0.75 mitoses / high power field (HPF). Using PHH3, the average rate was 1.33 mitoses / HPF. Mitotic rate by PHH3 was closely associated with mitotic rate by H&E ($p<0.01$ by linear regression), and was associated with the endpoint of metastasis at a higher significance level than was mitotic rate by H&E ($p=0.009$ for PHH3 vs. $p=0.05$ for H&E).

Conclusions: PHH3 allows for time-efficient determination of mitotic rate in malignant melanoma, correlates well with the H&E count, and can be particularly useful in cases with a brisk lymphocytic infiltrate or with numerous apoptotic or necrotic cells. In the studied cases, mitotic rate by PHH3 was a better predictor of metastasis than mitotic rate by H&E. Further study is warranted to determine the role of PHH3 in the routine examination of malignant melanoma cases.

1648 Validation of a Multiplex PCR Assay for Microsatellite Instability (MSI) Analysis: Evaluation of MSI in Sporadic Colorectal Cancer

WW Zhang, V Moroz, M Goodarzi, RK Yantiss, H Rennert. Weill Cornell Medical College, NY, NY.

Background: MSI characterizes hereditary non-polyposis colon cancer (HNPCC), and occurs in about 15% of sporadic colorectal cancer (CRC). A reference panel comprising 2 mononucleotide and 3 dinucleotide repeat markers was recommended by the National Cancer Institute (NCI) in 1997 to diagnose MSI. However, dinucleotide repeat markers are less sensitive and specific than mononucleotide repeat markers. Revised Bethesda Guidelines published by the NCI in 2002 recommended the usage of five quasimonomorphic mononucleotide repeat markers. We implemented a fluorescent multiplex PCR-based assay for detection of MSI using five mononucleotide repeat markers and studied MSI status in CRC.

Design: Multiplex MSI Assay DNA was extracted from routinely processed, formalin-fixed, paraffin embedded tissue sections of tumor and normal colon. Multiplex PCR was performed by amplifying 5 mononucleotide and 2 highly polymorphic pentanucleotide repeat markers (Promega MSI Analysis System). The PCR products were analyzed on an ABI 3100 Genetic Analyzer. Cases that showed MSI at one or two or more markers were interpreted to show low- and high-frequency MSI (MSI-L and MSI-H), respectively. Other cases were considered microsatellite stable (MSS). Validation of the MSI Assay and evaluation of MSI status in sporadic CRC 1. MSI validation studies were performed using a validation panel comprised of 8 tumors and the matching non-tumor tissues obtained from our laboratory and a reference laboratory. 2. MSI was evaluated in CRC samples obtained from 41 patients. The MSI data were compared to the results of immunohistoechemical stains (hMLH1, hMSH2, hMSH6) performed using standard techniques.

Results: 1. There was 100% concordance between our results and the validation panel results: 5 cases were MSI-H and 3 were MSS. 2. MSI analysis demonstrated MSI-H in 3/41 (7%) cases of CRC. 3. All three cases identified as MSI-H by MSI analysis showed immunohistochemical evidence of MSI.

Conclusions: The multiplex monoucleotide marker panel is a highly sensitive and specific test for MSI. Co-amplification of highly polymorphic pentanucleotide repeat markers insures sample identity.

1649 Patch Tissue Microarray (TMA): A Novel Technique for Tma Construction Using Pre-Existing Slides as a Source of Tissue When Paraffin Blocks Are Unavailable

Y Zhao, X Kong, M Ksionsk, P Lee, MB Bannan, J Melamed. New York University School of Medicine, New York, NY.

Background: TMA technology achieves miniaturization of samples permitting entire studies to be performed on single slides. This is increasingly becoming the preferred platform for tissue based research studies. TMA construction however has required access to the paraffin block to enable needle core extraction from the tissue. Institutions that treat referral patients receive consultation slides from many different hospitals and laboratories, but as they do not have possession of the original paraffin block are precluded from including these cases in research studies. We describe a technique for construction of TMA slides based on transfer of tissue from pre-existing routine slides instead of from the original paraffin blocks.

Design: As proof of this technique, we constructed a 20 core prostate cancer TMA from radical prostatectomy slides instead of from paraffin blocks. Briefly, this technique entails removal of the coverslip on each slide and reinforcement of the tissue by covering with Mount-Quick liquid mounting medium. Once the medium has hardened, the coverslip with attached tissue is punched using a tissue microarray needle. The removed biopsy disks are arrayed on an adhesive tape and then transferred and adhered to a recipient slide. For this technique to be useful, we wished to demonstrate that morphology was not compromised and that the tissue was sufficiently adherent to the slide to enable immunohistochemical staining. We therefore subjected a patch TMA with a traditional TMA on the same slide to immunohistochemical staining (34BE12) with antigen retrieval, and compared for expression of antigen and loss of cores.

Results: After immunohistochemical staining, morphology was equally preserved on both types of TMA with only slightly greater tissue loss on the patch TMA (19 of 20 cores intact on the traditional TMA compared with 16 of 20 cores intact on patch TMA). Expression of the immunohistochemical marker (34BE12) was equally specific on both TMAs.

Conclusions: Patch TMA represents a viable solution for TMA construction when paraffin blocks are unavailable. This technique, although laborious and with a limited output, is still valuable in allowing use of material for studies which otherwise would not be possible in the absence of paraffin embedded tissue. This may prove a useful technique at referral institutions where slides sent for review are the only tissue available.

Ultrastructural

1650 Electron Microscopic Findings in Skin Biopsies from Patients with Infantile Osteopetrosis and Neuronal Storage Disease

J Alroy, R Pfannl, A Ucci, A Pangrazio, F Rucci, A Frattini, A Megarbane. Tufts New England Medical Center, Boston, MA; Istituto Technologie Biomediche, Milano, Italy; Saint Joseph University, Beirut, Lebanon.

Background: Infantile osteopetrosis with neuronal storage is a rare lysosomal disease with early clinical manifestations that resemble some other lysosomal diseases. To date 51 different lysosomal diseases have been identified. Electron microscopic examination of skin biopsy is a cost effective screening tool for diagnosis of lysosomal storage diseases (J Child Neuro 11:301,1996). Skin biopsies from patients with infantile osteopetrosis with neuronal storage have not previously been described.

Design: Skin biopsies obtained from 1 month affected boy and his twin sister their family has a history of severe infantile autosomal recessive osteopetrosis. A biopsy was also obtained from 3 and a half months old boy. Molecular biology studies revealed unique mutations of *OSTM1* gene in each of the boys. The biopsies were fixed in Trumps fixative, post-fixed with osmium tetroxide, embedded in Epon, cut and stained with uranyl acetate and led citrate, and examined with Phillips EM 201.

Results: The skin biopsies of the normal and affected children contains epidermis, vascular endothelium, pericytes, fibroblasts, eccrine gland ducts, mast cells, macrophage, smooth muscle cells, nerves with myelinated and unmyelinated axons, Schwanns cell and perineural cells. The skin morphology of the twin sister appears to be normal. The biopsies of both boys revealed secondary lysosomes containing lipofuscin in Schwanns cells and endothelial cells, swollen axons, irregular thin myelinated sheaths and unmyelinated axons that contains spheroid inclusions.

Conclusions: The morphological changes seen in skin biopsies of infants with infantile osteopetrosis with neuronal storage due to mutation in *OSTM1* gene are unique and are different fromthose previously reported in skin biopsies of patients with other lysosomal storage disease.

1651 Intraneural Perineurioma: Meta-Analysis with Illustrative Cases

BL Boyanton, Jr, JK Jones, MJ Hicks, SM Shenaq, MB Bhattacharjee. Baylor College of Medicine, Houston, TX; University General Hospital, Houston, TX.

Background: Intraneural perineurioma (INP) may be confused with other "onion-bulb" Schwann cell entities (localized hypertrophic neuropathy-LHN, reactive/demyelinating processes, or inherited polyneuropathies of Charcot-Marie-Tooth/Dejerine Sottas) due to similar clinical, radiologic, and histologic features. The nerve is expanded by concentric whorls of spindle-shaped perineurial or Schwann cells, which can only be differentiated by ultrastructure (US) and immunohistochemsitry (IHC).

Design: Meta-analysis was performed on definitive INPs obtained via Medline. Inclusion criteria were a) nerve expansion by concentric whorls of spindle-shaped perineurial cells with thin elongated eosinophilic, cytoplasmic processes; b) epithelial membrane antigen (EMA) positive, S-100 protein negative; and/or c) US confirmed perineurial lineage (thin cytoplasmic processes, incomplete basal lamina, poorly formed tight junctions, pinocytotic vesicles). Baylor College of Medicine-affiliated hospitals databases yielded illustrative INP cases (n=2).

Results: Based upon IHC and/or US features, 53 INPs were identified (23M, 29F). Mean age was 23 years (range 2 to 64); 87% from patients ≤39 years. Affected nerves/sites (decreasing frequency) were ulnar, median, peroneal, posterior interosseous, sciatic, radial, brachial plexus, femoral, tongue, and tibial. Mean tumor size was 5.4 cm (range 0.5 to 18). No trauma preceding tumor diagnosis was noted in 37 cases; 16 cases did not comment on trauma history. Mean symptom duration was 53 months (range 2 to 300). Motor abnormalities were present in 43 cases, and absent or not reported in 5 cases each. Mean follow-up was 20 months (range 1 to 72). Surgical resection with nerve grafting or anastomosis resulted in motor improvement in most cases. Molecular features repeatedly showed monosomy of 22q and deletions of 22q11. Recurrences or metastasis were not reported. Only one patient had neurofibromatosis (NF).

Conclusions: INP is a neoplastic proliferation of perineurial cells with unique IHC (EMA positive, S100 negative) and ultrastructural (perineurial cell lineage) features. INP is distinct from other "onion-bulb" Schwann cell-derived entities (S100 positive, EMA negative). Despite unique molecular characteristics, INP has not been associated with NF. In conclusion, INP is a benign peripheral nerve sheath tumor, which does not recur or metastasize.

1652 Pathogenesis of Fibrillary Glomerulopathy (FG) with Emphasis on Ultrastructural Findings

GM Crisi, G Nunnemacher, J Isaac, GA Herrera. Baystate Medical Center/Tufts University School of Medicine, Springfield, MA; University of Utah Health Sciences Center, Salt Lake City, UT; Saint Louis University Medical Center, St. Louis, MO.

Background: The pathogenesis of FG remains controversial. Although the hypothesis that it represents an immune complex-mediated process is favored, this is not universally accepted. Characteristics of this renal-limited disorder include Congo red negativity, randomly disposed 15 to 25 nm in diameter fibrils containing amyloid-P component in various glomerular locations and rarely, along tubular basement membranes.

Design: Twenty FG cases were analyzed taking into account clinical histories, light microscopy (LM), immunofluorescence (IF) with routine battery of stains and EM findings to identify clues that would help in defining the pathogenesis of this disorder. The clinical presentation was primarily proteinuria. Two of the cases had documented diagnoses of systemic lupus erythematosus (SLE), 1 had antiphospholipid antibody syndrome, 2 diabetes mellitus and 2 plasma cell dyscrasias. One of these patients with SLE and FG, developed renal failure, was transplanted and in the allograft a classical lupus nephritis appeared.

Results: The LM appearance resembled a variety of glomerulopathies. Fourteen of 19 cases showed staining for both kappa and lambda light chains (74%) and in 17 ribbon-like IgG and C3 fluorescence was identified (89%). Four cases revealed "full-house" staining (21%) and 5 kappa restriction (26%). Ten of 20 cases revealed fibrils in mesangial areas and along peripheral capillary walls (50%) and 10 showed a "membranous" pattern with epi/intramembranous fibrillary deposits (50%), coexisting with immune complex type of deposits. Immunogold labeling for amyloid- P component in 2 cases showed colocalization with the fibrils.

Conclusions: The presence of both kappa and lambda light chains in association with the fibrillary deposits in the great majority of the cases, the coexistence of typical immune complexes with fibrils in cases with a membranous glomerulopathy pattern, and the identification of FG in the clinical setting of active SLE with IF and distribution of deposits most consistent with lupus nephritis, strongly supports that the fibrils represent polymerized immune complexes. The finding of kappa restriction in a few FG cases indicates that monoclonal light chains can also polymerize into fibrils. The specific mechanism/s responsible for fibrillogenesis may be related to the milieu and/or the presence of amyloid-P component in the deposits.

1653 A Rapid Method for Negative Staining of Fecal Samples for Diagnosis of Viral-Induced Gastroenteritis by Transmission Electron Microscopy

J Hicks, S-H Zhu, J Barrish. Texas Children's Hospital/Baylor College of Medicine, Houston, TX.

Background: Common etiologic agents for viral gastroenteritis are rotavirus, adenovirus, and "small round structure viruses" (enterovirus, Norwalk virus, calicivirus, astrovirus). Rapid viral infection diagnosis can avoid unnecessary antibiotic therapy, extensive costly medical workups and reduce hospital stays. Pseudo-replication for identifying viruses concentrates viral particles, but also concentrates fecal debris, making the screening process difficult and time consuming.

Design: A rapid negative staining method for viral particle identification in fecal samples is presented (modified Cubitt), that reduces debris and improves viral particle staining, while concentrating viral particles. This method requires <1ml of stool and may be prepared in <3m. Method is as follows: 1) Place small portion (0.5cm) of stool on glass slide/dish; 2) Add few drops of 2% phosphotungstic acid (pH 7.3) and mix thoroughly with stool; 3) Place drop of mixture on carbon-coated grid for 1m; 4) Remove as much fluid from grid as possible by touching torn edge of filter paper; 5) Before grid dries, place fresh drop of PTA on grid for 15-20s; 6) Remove excess fluid by gently touching grid to torn edge of filter paper. Allow grid to air-dry; 7) Examine grid for viral particles.

Results: To compare the modified Cubitt method of negative staining for stool samples to the pseudo-replica technique, 25 known samples of rotavirus, adenovirus, picornaviruses and negative controls were prepared by both methods. Each preparation was screened for 15m. Viral particles were counted per grid square and then rated as 1+, 2+ or 3+. Of the 14 positive samples, the modified Cubitt method was more sensitive than pseudo-replica with 10 of 14 samples and equally sensitive in 2 of 14 samples.

Conclusions: The rapid negative staining method for fecal sample preparation is preferable to the pseudo-replica technique for several reasons. This modified Cubitt method provides improved viral particle detection due to decreased background fecal debris and enhanced viral particle staining. The etiologic agent for viral gastroenteritis